AD-A186 889 INVESTIGATION OF THERMOACOUSTIC HEAT TRANSPORT USING A THERMOACOUSTIC COUPLE(U) NAVAL POSTGRADUATE SCHOOL MONTEREY CA M L MUZZERALL SEP 87 1/1

UNCLASSIFIED F/G 20/1 NL

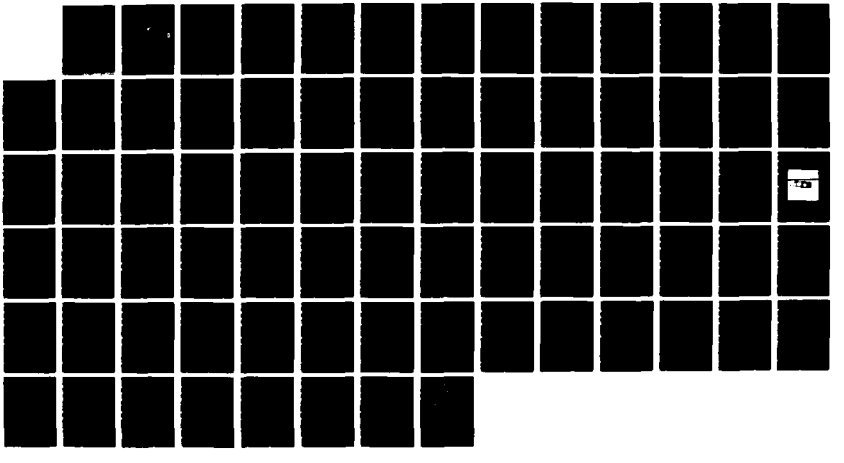

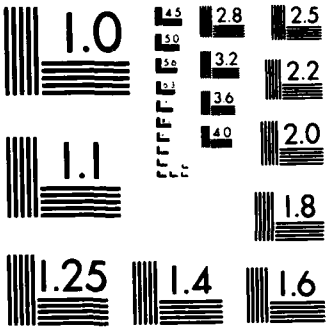

MICROCOPY RESOLUTION TEST CHART
NATIONAL BUREAU OF STANDARDS 1963-A

NAVAL POSTGRADUATE SCHOOL

Monterey, California

THESIS

INVESTIGATION OF THERMOACOUSTIC HEAT TRANSPORT
USING A THERMOACOUSTIC COUPLE

by

Michael Louis Muzzerall

September 1987

Thesis Advisors: A.A. Atchley
T.J. Hofler

UNCLASSFIED
SECURITY CLASSIFICATION OF THIS PAGE

ADA186889

REPORT DOCUMENTATION PAGE

1a REPORT SECURITY CLASSIFICATION UNCLASSIFIED	1b RESTRICTIVE MARKINGS
2a SECURITY CLASSIFICATION AUTHORITY	3 DISTRIBUTION/AVAILABILITY OF REPORT Approved for public release; distribution is unlimited.
2b DECLASSIFICATION/DOWNGRADING SCHEDULE	
4 PERFORMING ORGANIZATION REPORT NUMBER(S)	5 MONITORING ORGANIZATION REPORT NUMBER(S)
6a NAME OF PERFORMING ORGANIZATION Naval Postgraduate School 6b OFFICE SYMBOL (If applicable) Code 61	7a NAME OF MONITORING ORGANIZATION Naval Postgraduate School
6c ADDRESS (City, State, and ZIP Code) Monterey, California 93943-5000	7b ADDRESS (City, State, and ZIP Code) Monterey, California 93943-5000
8a NAME OF FUNDING/SPONSORING ORGANIZATION 8b OFFICE SYMBOL (If applicable)	9 PROCUREMENT INSTRUMENT IDENTIFICATION NUMBER
8c ADDRESS (City, State, and ZIP Code)	10 SOURCE OF FUNDING NUMBERS PROGRAM ELEMENT NO / PROJECT NO / TASK NO / WORK UNIT ACCESSION NO

11 TITLE (Include Security Classification)
Investigation of Thermoacoustic Heat Transport Using a Thermoacoustic Couple

12 PERSONAL AUTHOR(S)
Muzzerall, Michael L.

13a TYPE OF REPORT	13b TIME COVERED FROM TO	14 DATE OF REPORT (Year Month Day)	15 PAGE COUNT
Masters Thesis		1987 September	75

16 SUPPLEMENTARY NOTATION

17 COSATI CODES			18 SUBJECT TERMS (Continue on reverse if necessary and identify by block number)
FIELD	GROUP	SUB GROUP	Acoustics, Thermoacoustics, Thermoacoustic heat transport

19 ABSTRACT (Continue on reverse if necessary and identify by block number)

The results of measurements of thermoacoustically generated temperature gradients in short, thin plates located in a resonant tube are reported. The temperature gradient results from a heat flow generated by the acoustic field. Measurements, at both axial and transverse positions in the tube, are made for pressure amplitudes ranging from approximately 145 dB to 162 dB re 20 uPa (rms), in argon and helium, for single plates and stacks of up to five plates having separations from approximately 4 to 40 thermal penetration

20 DISTRIBUTION/AVAILABILITY OF ABSTRACT	21 ABSTRACT SECURITY CLASSIFICATION	
☒ UNCLASSIFIED/UNLIMITED ☐ SAME AS RPT ☐ DTIC USERS	UNCLASSIFIED	
22a NAME OF RESPONSIBLE INDIVIDUAL Anthony A. Atchley	22b TELEPHONE (Include Area Code) 408-646-2848	22c OFFICE SYMBOL 61 AY

DD FORM 1473, 84 MAR 83 APR edition may be used until exhausted
All other editions are obsolete

SECURITY CLASSIFICATION OF THIS PAGE
UNCLASSFIED

19. ABSTRACT (continued)

depths. The results are compared to predictions based upon a theory by Wheatley and others (J. Wheatley, et al., Journal of the Acoustical Society of America, Vol. 74, pp. 153-170, 1983). For pressure amplitudes below 150 dB, the measurements agree with theory. At higher pressure amplitudes, the agreement diminishes. It is concluded that non-thermal effects are responsible for the discrepancies.

Approved for public release; distribution is unlimited.

Investigation of Thermoacoustic Heat Transport Using a Thermoacoustic Couple

by

Michael Louis Muzzerall
Captain, Canadian Forces
B.Sc., Royal Military College of Canada, 1975

Submitted in partial fulfillment of the requirements for the degree of

MASTER OF SCIENCE IN ENGINEERING ACOUSTICS

from the

NAVAL POSTGRADUATE SCHOOL
September 1987

Author: _____
Michael Louis Muzzerall

Approved by: _____
Anthony A. Atchley, Thesis Advisor

_____
Thomas J. Hofler, Thesis Co-Advisor

_____
Steven L. Garrett, Chairman,
Engineering Acoustics Academic Committee

_____
G. E. Schacher, Dean of Science and Engineering

ABSTRACT

The results of measurements of thermoacoustically generated temperature gradients in short, thin plates located in a resonant tube are reported. The temperature gradient results from a heat flow generated by the acoustic field. Measurements, at both axial and transverse positions in the tube, are made for pressure amplitudes ranging from approximately 145 dB to 162 dB re 20 μPa (rms), in argon and helium, for single plates and stacks of up to five plates having separations from approximately 4 to 40 thermal penetration depths. The results are compared to predictions based upon a theory by Wheatley and others (J. Wheatley, et al., *Journal of the Acoustical Society of America*, Vol. 74, pp. 153–170, 1983). For pressure amplitudes below 150 dB, the measurements agree well with theory. At higher pressure amplitudes, the agreement diminishes. It is concluded that non-thermal effects are responsible for the discrepancies.

TABLE OF CONTENTS

ACKNOWLEDGMENT

I would like to thank my thesis advisors, Dr. Anthony Atchley and Dr. Thomas Hofler, for their assistance, words of wisdom, and infinite patience. Their gentle prodding made this subject interesting and much easier to understand. Without their capable hands, my ten thumbs and I would still be in the basic construction phase of the experiment.

Next, I thank Mr. George Jaksha of the physics department machine shop. His unparalleled ability and insight into sometimes poorly worded construction requests resulted in precisely made apparatus which enabled me to conduct my experiment.

Next, I thank my fellow students who endured many hours of high dBs while trying to study.

Finally, I thank my wife, Candyce. Her typing and editing skills allowed for timely completion of a readable thesis. More importantly, however, was her understanding of the many hours required for this project and her support through it all.

I. INTRODUCTION

Thermoacoustic heat transport has been studied in detail by the late John Wheatley and associates [Refs. 1 and 2]. One instrument developed in these studies is the thermoacoustic couple, or TAC. Wheatley found that, when a TAC is placed in a resonant tube, driven so that the acoustic wavelength is much greater than the length of the TAC, a temperature gradient is induced across it. The gradient is a function of the acoustic pressure amplitude, the type of gas in the tube, the thermodynamic properties of the TAC plate material, the length of the plate, and the plate configuration (i.e., single or multiple plates).

It is interesting that, while Wheatley states that the thermoacoustic phenomena can be observed in a single plate [Ref. 1:p. 155], his single plate results indicate a large deviation from theory [Ref. 1:p. 158]. This discrepancy is noted, but there is no report of further investigation into its cause.

The purpose of this thesis is to study the thermoacoustic effect, on a single plate and on multiple plates, to better understand both the basic theory of thermoacoustic heat transport and the reason for single plate discrepancies.

The results of two experiments are reported. In the first experiment, changes in the temperature difference across a TAC are studied as a function of the longitudinal position of the TAC in the resonant

tube, the number of plates in a stack, the spacing between plates, the acoustic pressure amplitude, and the type of gas in the tube. In the second experiment, the developed temperature difference is measured as the TAC position is varied along a diameter of the tube. The results of these experiments are compared to the theory as developed by Wheatley and associates. Possible causes for the observed deviations from theory are offered.

II. THEORY

A. INTRODUCTION

A synopsis of the theory of thermoacoustic heat transport, based upon John Wheatley's development, follows. In addition to the basic theory, modifications to account for the thermal conductivity of the gas will be considered. The possible effects that non-thermal processes may have on the heat transport will also be discussed. The reader is directed to References 1 and 2 for a more detailed development of the basic theory.

B. THERMOACOUSTIC EFFECT

1. Basic Theory

In order to understand the thermoacoustic effect, it is necessary to describe what happens to a gas parcel in an acoustic standing wave developed within a resonant tube. In this study, we are considering the heat pumping action of such an acoustic wave.

The four stages of the heat pumping cycle are depicted in Figure 1 [Ref. 2:p. 13]. Initially, let us assume that the plate, or TAC, has a small temperature gradient, ∇T, across it. Also, let us assume that the idealized plate does not conduct heat in the longitudinal x-direction. At step 1, a gas parcel undergoes an adiabatic compression from pressure p to $p+p_1$. At the same time, the parcel is displaced toward the pressure antinode by a distance x_1. This distance may be

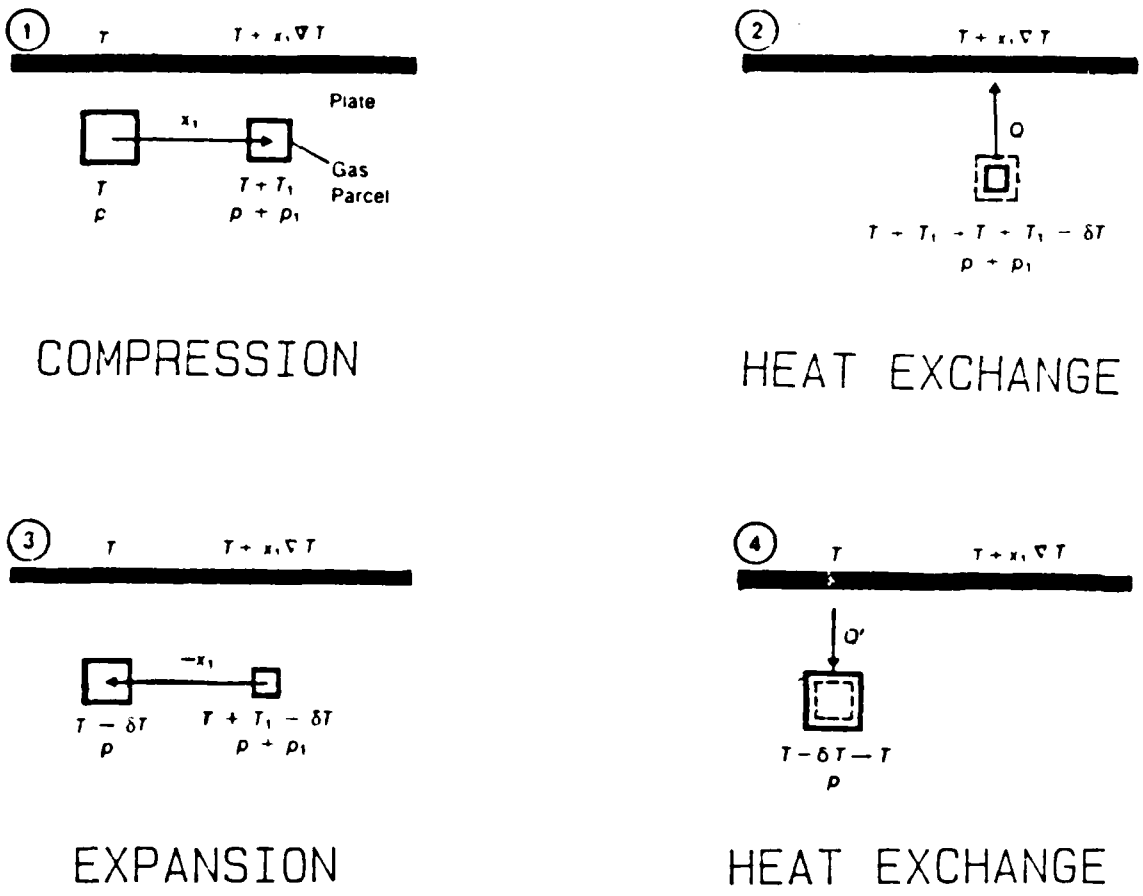

Figure 1 -The Thermoacoustic Heat Pumping Cycle

expressed as $x_1 = p_1/\rho_m c\omega$ where p_1 is the acoustic pressure or adiabatic pressure change, ρ_m is the density of the gas, c is the speed of sound in the gas, and ω is the angular frequency. Also, at this time, the parcel's temperature increases from T to $T+T_1$. T_1 is the adiabatic temperature change and will be discussed in more detail in the following pages. At step 2, there is a heat flow, Q, in the transverse direction, from the hotter gas volume to the cooler plate. This heat flow also results in a temperature reduction δT in the gas volume. On the return leg, step 3, the gas parcel expands adiabatically and moves back a distance x_1 but is now at a lower temperature $T-\delta T$. Therefore, at step 4, there is another heat exchange, Q', but this time from the hotter plate to the cooler gas. This heat exchange brings the gas back to the original temperature T while, at the same time, it reduces the temperature of this end of the plate. This heat pumping cycle repeats with the frequency of the acoustic wave.

In describing the heat flow in short stacks associated with this process, Wheatley, et al., estimate the hydrodynamically transported heat Q" as

$$Q'' \sim \Pi \, \delta_\kappa \, u_1 \, c_p \, \rho_m \, \delta T \qquad (1)$$

[Ref 2:p. 14], where

Π = overall perimeter of the plate (measured transverse to the flow);
δ_κ = thermal penetration depth;
u_1 = acoustic velocity magnitude;
c_p = specific heat at constant pressure of the gas; and

δT = change in temperature in the gas due to the heat flow process. From Figure 1, step 2, it can be seen that

$$\delta T = T_1 - x_1 \nabla T = T_1 \left(1 - \frac{\nabla T}{T_1/x_1}\right). \tag{2}$$

T_1, as earlier stated, is the adiabatic temperature change, and may be expressed by

$$T_1 = \frac{T_m \beta}{\rho_m c_p} p_1 \tag{3}$$

where

T_m = mean absolute temperature; and
β = isobaric expansion coefficient.

For an ideal gas, the product $T_m\beta$ equals unity.

The value for ∇T which makes $\delta T = 0$, in equation 2, is known as the critical gradient so that

$$\nabla T_{crit} = \frac{T_1}{x_1} \tag{4}$$

[Ref. 2:p. 14]. This temperature gradient is the largest that can be acoustically induced on this plate.

Using Wheatley's definition $\Gamma \equiv \nabla T / \nabla T_{crit}$ [Ref. 2:p. 14] and rearranging the terms in equation (1), we can express the hydrodynamic heat flow as

$$Q'' \sim \Pi \delta_\kappa (T_m \beta) p_1 u_1 (1 - \Gamma). \tag{5}$$

For the assumed ideal plate, we will remain in the heat pumping regime while the heat flow is towards the nearest pressure antinode. This will occur as long as $\nabla T < \nabla T_{crit}$ or $\Gamma < 1$. If $\nabla T = \nabla T_{crit}$, then there is no heat flow.

Now, let us consider that the TAC is not ideal and, thus, does conduct heat. There now exists a return heat flow Q_r, due to diffusive thermal conduction through the plate material. This heat flow may be expressed as $Q_r = \kappa A \nabla T$, where κ is the thermal conductivity in the direction of the plate length, A is the area of the plate transverse to the flow, and ∇T is the temperature gradient across the plate. The net heat flow of this system, Q_t, may be expressed as

$$Q_t = Q'' - Q_r, \tag{7}$$

or

$$Q_t = \left[\Pi \delta_\kappa (T_m \beta) p_1 u_1 (1 - \Gamma)\right] - [\kappa A \nabla T]. \tag{8}$$

Considering this heat flow, the heat pumping regime is maintained as long as Q'' is directed toward the nearest pressure antinode. At $Q'' = Q_r$, we have reached steady state and $Q_t = 0$. We have, then, the maximum temperature gradient, ∇T, of this system. For a given transverse area A, a non-zero κ will limit the maximum value of the temperature gradient to that achieved when $Q'' = Q_r$.

Now, consider the term $\Pi \delta_\kappa (T_m \beta)$ as constant for any position of the TAC in the standing wave. This results in Q'' being dependent on the $p_1 u_1 (1 - \Gamma)$ product. [For small acoustic amplitudes, ∇T

is small, $\Gamma \approx 0$, and thus $(1 - \Gamma) \rightarrow 1$ and is inconsequential. At large amplitudes, ∇T approaches ∇T_{crit} and $(1 - \Gamma) \rightarrow 0$. This will affect $\dot{Q}''$. These two cases will be discussed in more detail later in this paper.] By studying equation 8, we can see that, for a given κ and plate geometry, the temperature gradient that exists across the TAC, in the heat pumping case, is dependent on the p_1u_1 product.

The acoustic amplitude p_1 and particle velocity u_1 vary with position in the standing wave. They may be expressed as

$$p_1 = P_0 \cos (kx) \tag{9}$$

and

$$u_1 = U_0 \sin (kx), \tag{10}$$

where k is the wave number, x is the displacement from the closed end of the tube, and P_0 and U_0 are the magnitudes of the pressure and velocity at their respective antinodes. Thus the product p_1u_1 may be expressed as

$$p_1u_1 = \left[\frac{(P_0\, U_0)}{2} \sin (2kx)\right]. \tag{11}$$

The temperature gradient, therefore, can be expected to vary sinusoidally. Figure 2, although not to scale, shows the relationship among p_1, u_1, and ∇T plus the variation of ∇T_{crit}. As is evident, the temperature gradient swings from positive to negative values with zeroes at either the pressure or velocity nodes. This brings us to the point that the heat flow is towards the nearest pressure antinode.

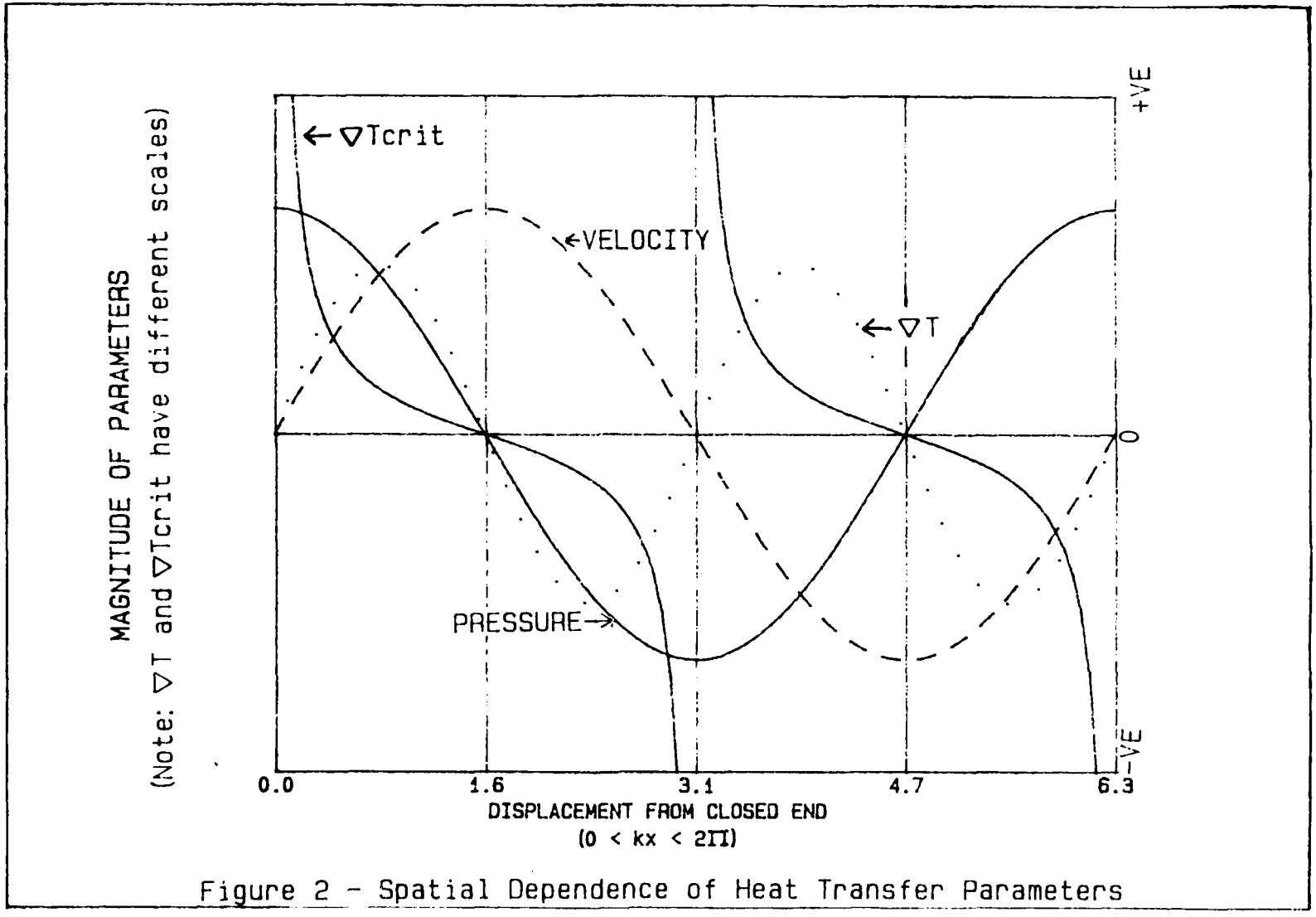

Figure 2 - Spatial Dependence of Heat Transfer Parameters

This is expected because, as a parcel of gas is moved, in the positive x-direction, toward a pressure antinode (Figure 1), the parcel is compressionally warmed and thus will transfer heat to the plate. If the parcel is moved toward a pressure node, it experiences cooling by expansion and takes heat from the plate. Furthermore, from equation (8) and Figure 2, we deduce that as $\nabla T_{crit} \rightarrow 0$ the temperature gradient itself must approach zero.

In our investigation, the plate and gas will initially be at the same temperature. At the onset of the acoustic pressure $\Gamma = 0$ and, therefore, as seen by equation (5), the heat flow is initially a maximum. This will result in a temperature gradient across the plate which will increase toward ∇T_{crit}. However, as discussed in equations (7) and (8), ∇T will increase only until steady state is achieved, i.e., $Q_r = Q''$.

In Ref. 1 (pp. 155–157), Wheatley, et al., discuss the aforementioned heat flow in a slightly different manner. There, the development is continued in order to derive an expression with which to calculate the temperature difference developed across a TAC. That expression is:

$$\Delta T = \frac{\left[\dfrac{\left(.25\, P_0^2\, \delta_\kappa\, (1 + \sigma^{1/2})\right)}{\left(\rho_m c\, (\kappa d_2/L)\, (1 + \sigma)\right)} \sin\,(2\omega x/c)\right]}{\left[\dfrac{\left(1 + P_0^2\, \delta_\kappa\, (1 - \sigma^{3/2})\right)}{\left(4(\kappa d_2/L)\rho_m L T_m \omega\, (\gamma - 1)\, (1 - \sigma^2)\right)} \left[1 - \cos(2\omega x/c)\right]\right]} \qquad (12)$$

[Ref. 1:p. 157, Eqn. 17], where

ΔT = temperature difference across the plate
P_0 = peak acoustic pressure of the driver

δ_κ = thermal penetration depth
σ = Prandtl number of the gas
γ = the ratio C_p/C_v of the gas
L = length of the plate
T_m = mean ambient temperature
ρ_m = mean density of the gas
c = speed of sound in the gas
ω = angular frequency
x = mean position of TAC center measured from the closed end of the tube
κ = thermal conductivity of the plate
d_2 = thickness of the plate.

It is this equation and predictions based on it that will be examined in this thesis.

2. Surrounding Gas Considerations

In the preceding equation, the product κd_2 ignores the thermal return path via the gas surrounding the TAC. This return path is generally the gas between two plates. Therefore, the thickness of the gas path is equal to the plate separation. With a stack of plates, this path is well defined and can be expressed as either the absolute distance between the plates or as a multiple of the thermal penetration depth. Thus, we can express the effective κd_2 for a stack of plates as:

$$\kappa d_2 = (\kappa_g * \text{separation}) + (\kappa_p * d_2), \tag{13a}$$

or

$$\kappa d_2 = (\kappa_g * \delta_\kappa * N) + (\kappa_p * d_2), \tag{13b}$$

where N is the number of thermal penetration depths equivalent to the required separation and κ_g and κ_p are the thermal conductivities of the gas and plate, respectively.

For a single plate, the return path is not as well defined. In order to estimate the effect of the thermal conduction through the gas, we consider two extreme cases. In the first case, the return path is assumed to be 5 thermal penetration depths above and below the plate, for a total of 10 penetration depths. In the second case, it is assumed that the nearest boundary is approximately one tube radius away and thus the effective thickness of the return path is one tube diameter. In other words, the majority of the space in the tube provides the return path. Using this assumption, the effective κd_2 becomes

$$\kappa d_2 = (\kappa_g * \text{Diameter}) + (\kappa_p * d_2). \qquad (14)$$

To avoid confusion between the two methods of including the gas return path, equations (13a) and (13b) will be referred to as Theory, while equation (14) will be referred to as Modified or Mod Theory. It is predicted that Theory underestimates the effect of the gas thermal conduction, while Mod Theory presents the absolute upper limit on the gas conduction.

C. TEMPERATURE DIFFERENCE PREDICTION

Now consider a single steel plate TAC, of length 2.26 cm, width 2.16 cm, and thickness 0.127 mm, placed in an Argon-filled tube at

294 K. The thermal conductivity of steel is 17 W/m-K [Ref. 3:p. D-187]. The tube is driven at 705 Hz at an acoustic pressure level of 150 dB re 20μPa, or approximately 600 Pa (rms). The gas return path thickness is assumed to be 5 thermal penetration depths for Theory and 6 cm for Mod Theory. Using these parameters and the properties of Argon [Ref. 4; see Appendix 1], the predicted temperature difference can be calculated from equation (12). As can be seen in Figure 3, Theory predicts a higher temperature difference than Modified Theory. This difference is expected since Mod Theory assumes a much larger volume of gas with which to conduct heat.

Consider now a stack of plates, with plate separation of 1 mm, placed in the same resonant tube filled with Argon at 294 K. This time, the acoustic pressures will be 150, 162, 168, and 174 dB re 20μPa. The predicted temperature differences are shown in Figure 4. As can be seen, the temperature difference developed across the TAC increases with increasing acoustic amplitude. At higher amplitudes, there is a tilting or skewing of the temperature curve toward the pressure antinode. In contrast, Figure 5 shows the effect of using Helium in the tube. The physical properties of this gas [Ref. 5:pp. 48-49] result in a much larger temperature difference at the same amplitudes and also lead to a much more noticeable skewing effect.

Returning to the discussion on heat flow, one can determine the origin of this skewing. In equation (8) and Figure 2, the effect of the product $p_1 u_1$ was seen. Near a pressure antinode, the pressure p_1 is large and thus gas parcels undergo a large temperature change due to

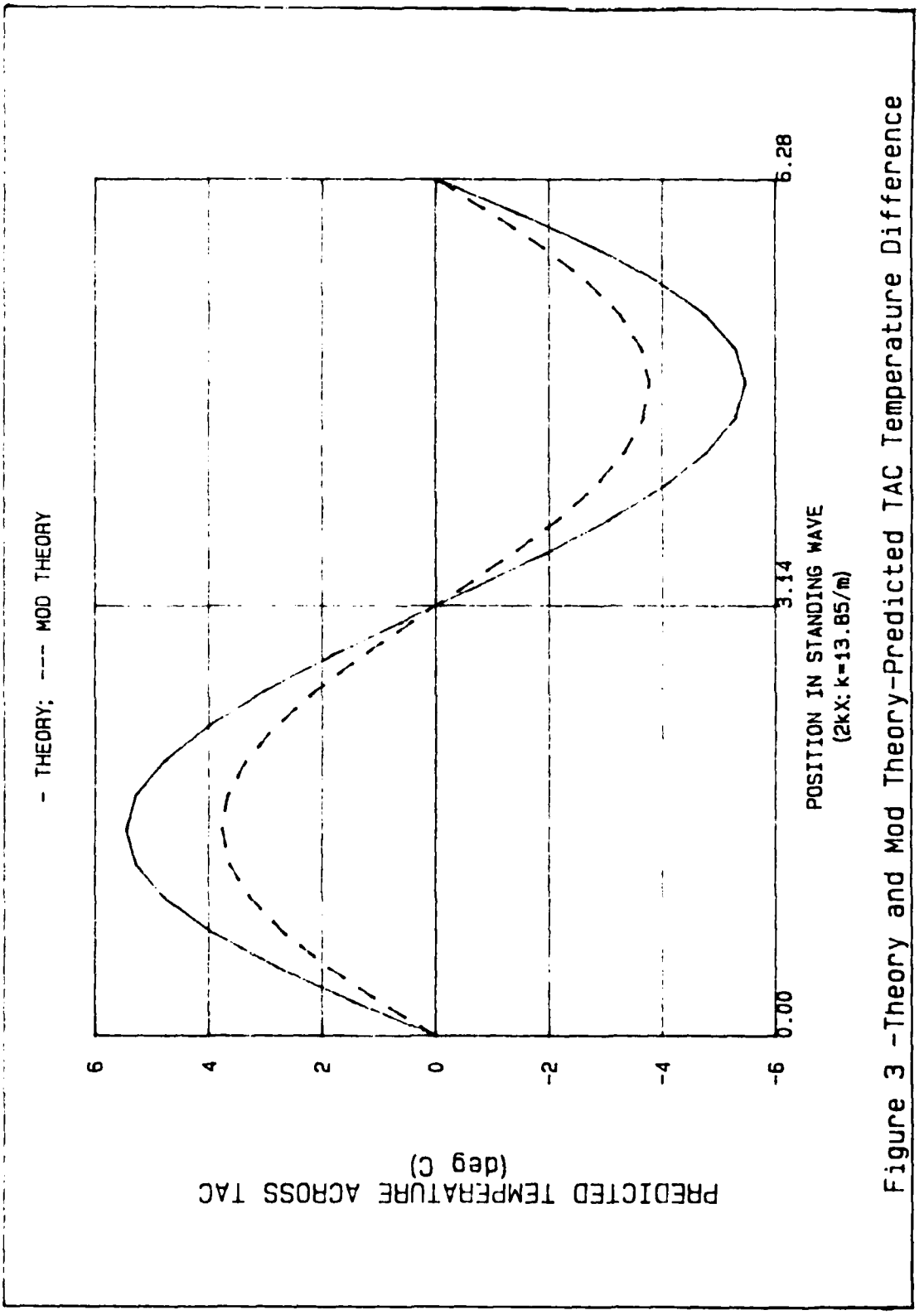

Figure 3 -Theory and Mod Theory-Predicted TAC Temperature Difference

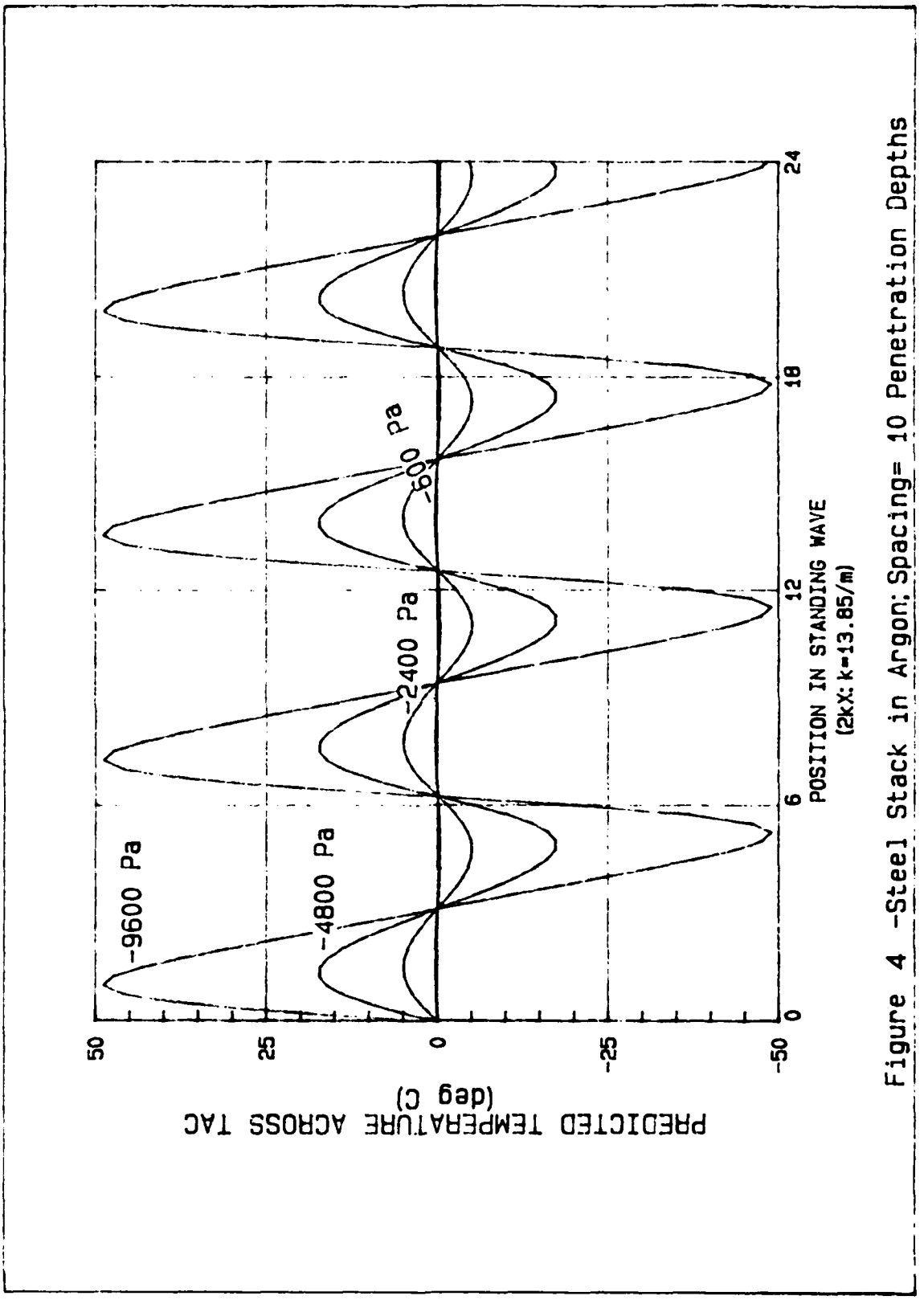

Figure 4 -Steel Stack in Argon; Spacing= 10 Penetration Depths

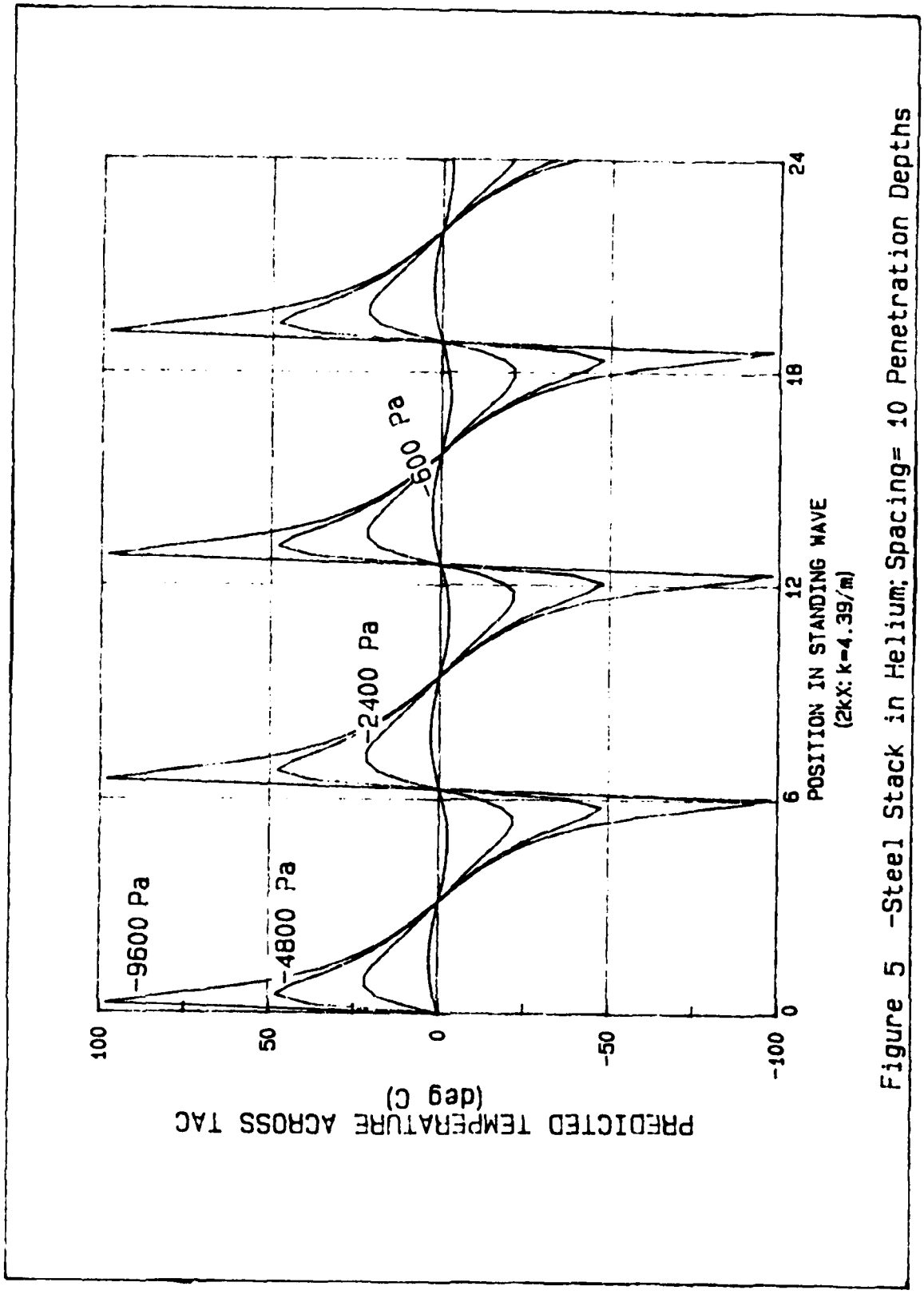

Figure 5 -Steel Stack in Helium; Spacing= 10 Penetration Depths

compression. At the same time, the displacement due to u_1 is small. This combination of a large temperature change over a small displacement means, by definition, that there is a large critical temperature gradient. This is confirmed by the large value of ∇T_{crit} near the pressure antinodes in Figure 2. This also explains the large temperature difference near the pressure antinodes observed in Figures 4 and 5. A large ∇T_{crit} would allow ∇T to increase via the $(1 - \Gamma)$ term in equation (8), and thus for a given TAC length the temperature difference would increase. Now, as the TAC is moved from the pressure antinode, the value of ∇T_{crit} decreases rapidly. This causes a rapid decrease in Q'', because of $(1 - \Gamma) \rightarrow 0$, and a corresponding rapid change in the developed temperature gradient is predicted. As a pressure node is approached, ∇T_{crit} approaches zero, but at a slow rate. Therefore, a much more gradual change in the temperature gradient is predicted. This means a corresponding gradual change in the temperature difference. Thus, we see that at higher pressure amplitudes we expect to see the skewing evident in Figures 4 and 5.

By considering the separation of the plates as a means to define a return path through the gas, it is evident that the predicted temperature difference will vary with plate separation. Furthermore, while it is not readily apparent from equation 12, Wheatley's group studied the rate of change in temperature on a stack of plates as it relates to plate separation distance d, compared to the viscous penetration depth distance δ_v. Their conclusion was that, "... qualitative changes from the simple boundary layer theory may begin to show up for $d < 2\delta_v$."

[Ref. 1:p. 155] We would, therefore, expect deviation from theory as the separation approaches the viscous penetration depth.

D. NON-THERMAL PROCESSES

In addition to the aforementioned thermal effects, there are other hydrodynamic effects due to the impinging acoustic wave. While these additional processes may have secondary thermal effects, they are non-thermal in origin and therefore are identified as non-thermal processes. In a standing wave tube which is driven at resonance, there is a streaming motion at the tube boundaries which is toward the velocity nodes as is depicted in Figure 6 [Ref. 6:p. 348]. As discussed earlier, the heat flow developed in this same tube is towards the same velocity nodes. If the TAC is on the longitudinal axis of the resonant tube, the acoustic streaming will provide an increase in the return heat flow. For a single plate, this additional return flow may cause the temperature gradient to be less.

For a stack of plates, the effects of streaming will depend on the effect that the additional plates have on the streaming pattern in the tube. The plate separation may also be important to the tube pattern. The one-way streaming that occurs over the individual plates may be more prominent than the tube effects. At this point, we can only say that acoustic streaming effects are difficult to predict but they are likely to occur at the pressure amplitudes typically used in the investigation of the thermoacoustic effect.

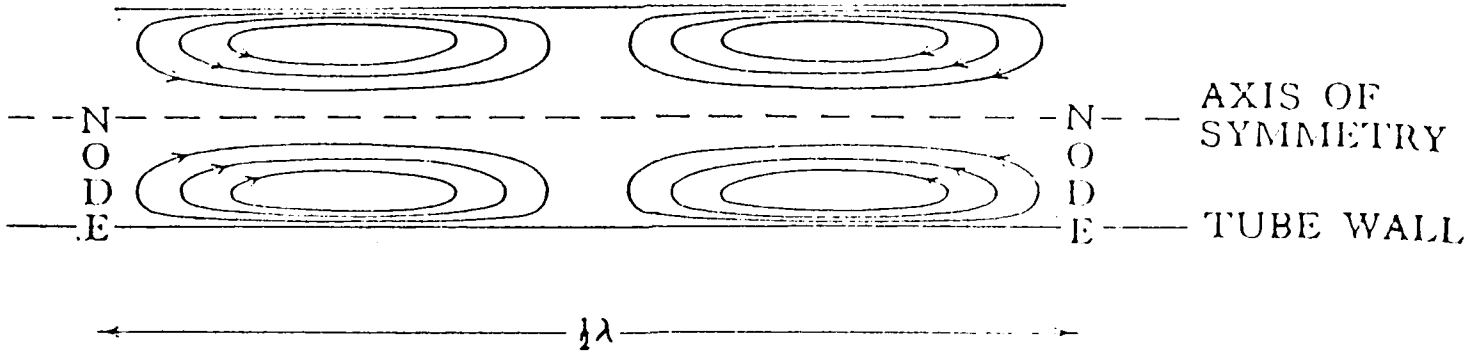

Figure 6 -Acoustic Streaming Pattern Between Velocity Nodes in a Resonant Tube

III. EXPERIMENTS

A. LONGITUDINAL MAPPING

In order to study the temperature variation with respect to position in a standing wave, a copper tube 89.7 cm in length and 6.22 cm in diameter was used as the resonant cavity. The tube was filled with Argon and pressurized to just above atmospheric pressure to ensure that all leaks would be outward. Figure 7 shows the equipment arrangement for this portion of the experimentation.

Before data acquisition began, the endplate and probe microphones were calibrated. The microphone at the endplate (Endevco, Model #8550M1) was used to accurately monitor the frequency and amplitude of sound in the tube. This microphone is readily calibrated using a D.C. calibration method (see Figure 8). The response of the microphone was assumed to be flat from D.C. to the experimental frequencies because the fundamental microphone resonance is at 50 KHz. The other microphone used was an earpiece from a portable television set. As this transducer was used only to monitor the position of the pressure extremes in the tube and not to determine absolute pressures, precise calibration was not required. Therefore, a rough comparison calibration using the Endevco as a standard was completed. Later, due to poor performance at high acoustic pressures, the earpiece was replaced by a similarly calibrated, locally constructed, piezoceramic transducer.

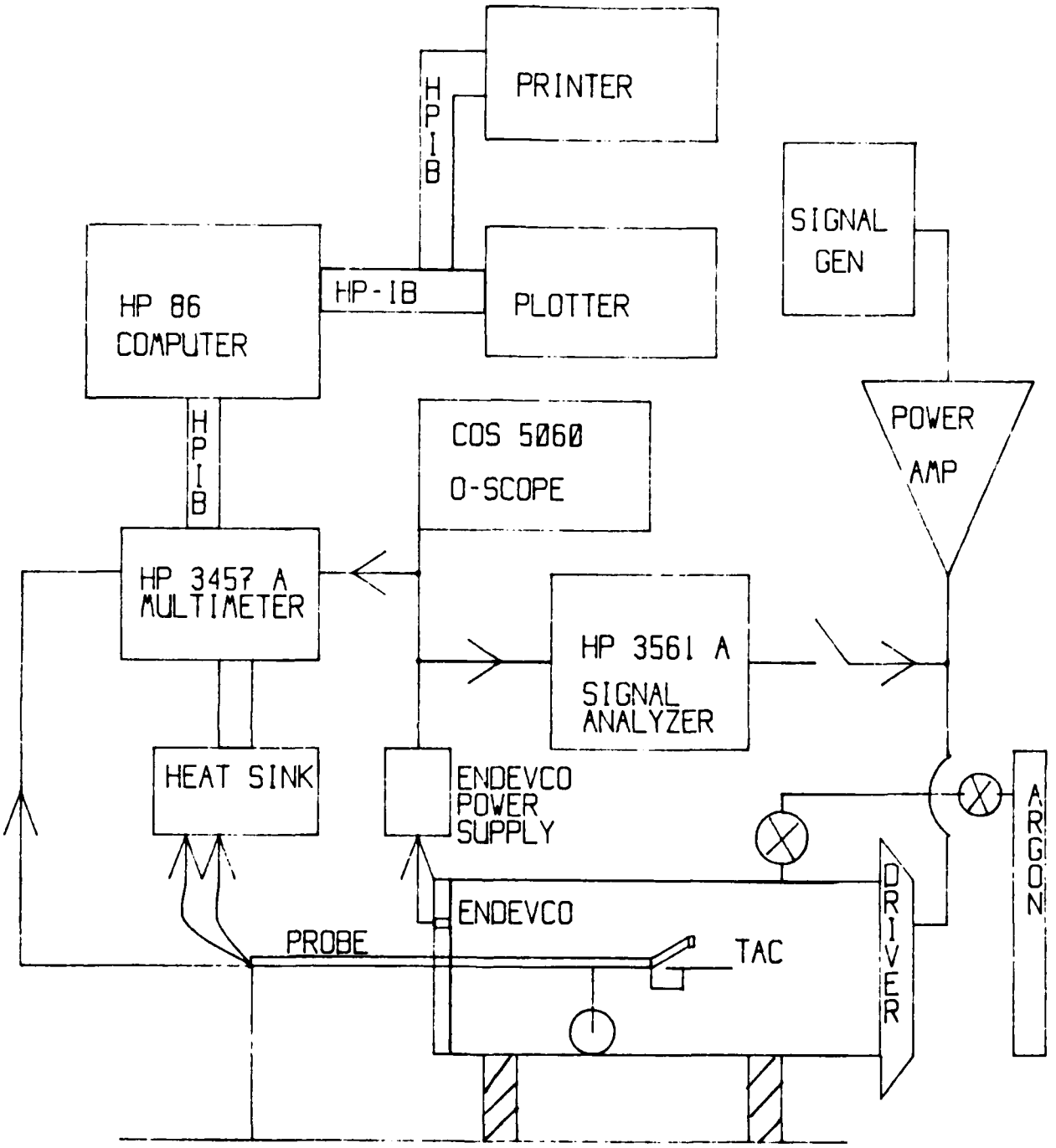

Figure 7 -Experimental Equipment Set-up

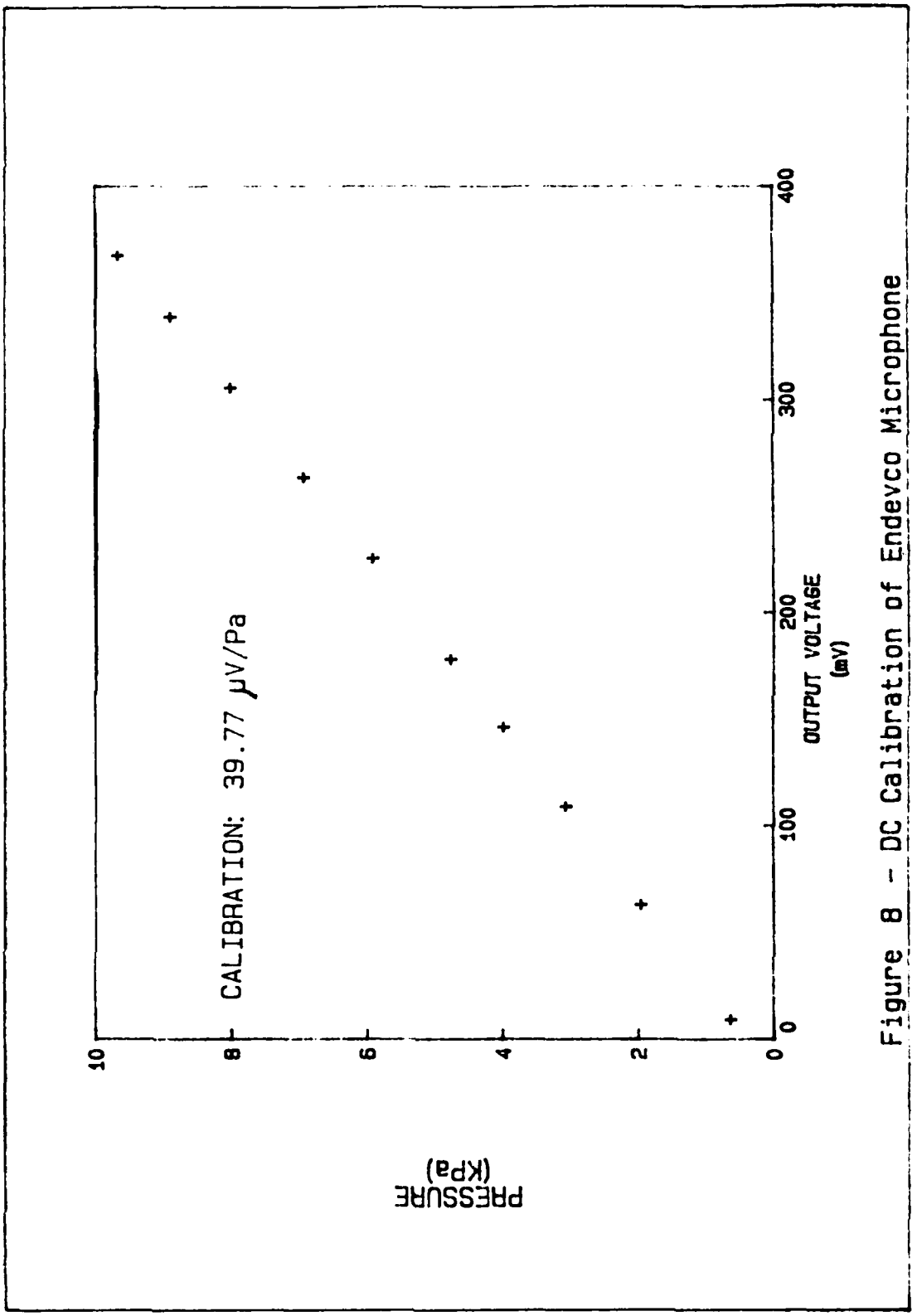

Figure 8 - DC Calibration of Endevco Microphone

To determine a suitable driving frequency, the resonances of the Argon-filled tube were studied (see Figures 9 and 10). An interesting point of this procedure was the discovery that the speed of sound in Argon of 319 m/s at 0° C, obtained from a well-used source [Ref. 3:p. E-47], is in error. By comparing the tube length to the observed resonant frequencies, the speed of sound was calculated to be near 320 m/s at 20° C. Further research found three more-recent sources [Ref. 4; Ref. 7:p. 3133; Ref. 8:p. 264] which give the value of 319 m/s at 20° C. This is the value used for the following experiments.

Using a single sheet glass TAC, trial runs were conducted to verify experimental procedures. This trial provided a method of determining the time required for stabilization of the TAC temperature after it had been moved (see Figure 11 for typical plot). This was required for the automation of data acquisition. Using the measured temperature gradient results from this trial run (Figure 12), a decision was made regarding the portion of the tube from which useful data could be obtained.

A TAC, consisting of one 0.0127 cm thick stainless steel sheet laminated to one 0.0127 cm thick G-10 fiberglass sheet, 2.26 cm long and 2.16 cm wide, was fitted with a thermopile consisting of four pairs of constantan-chromel thermocouples. To ensure correct voltage readings due to the temperature difference developed across the TAC, the leads from the TAC are put in thermal contact with a copper plate to provide a stable temperature reference (see Figure 7). This "heat

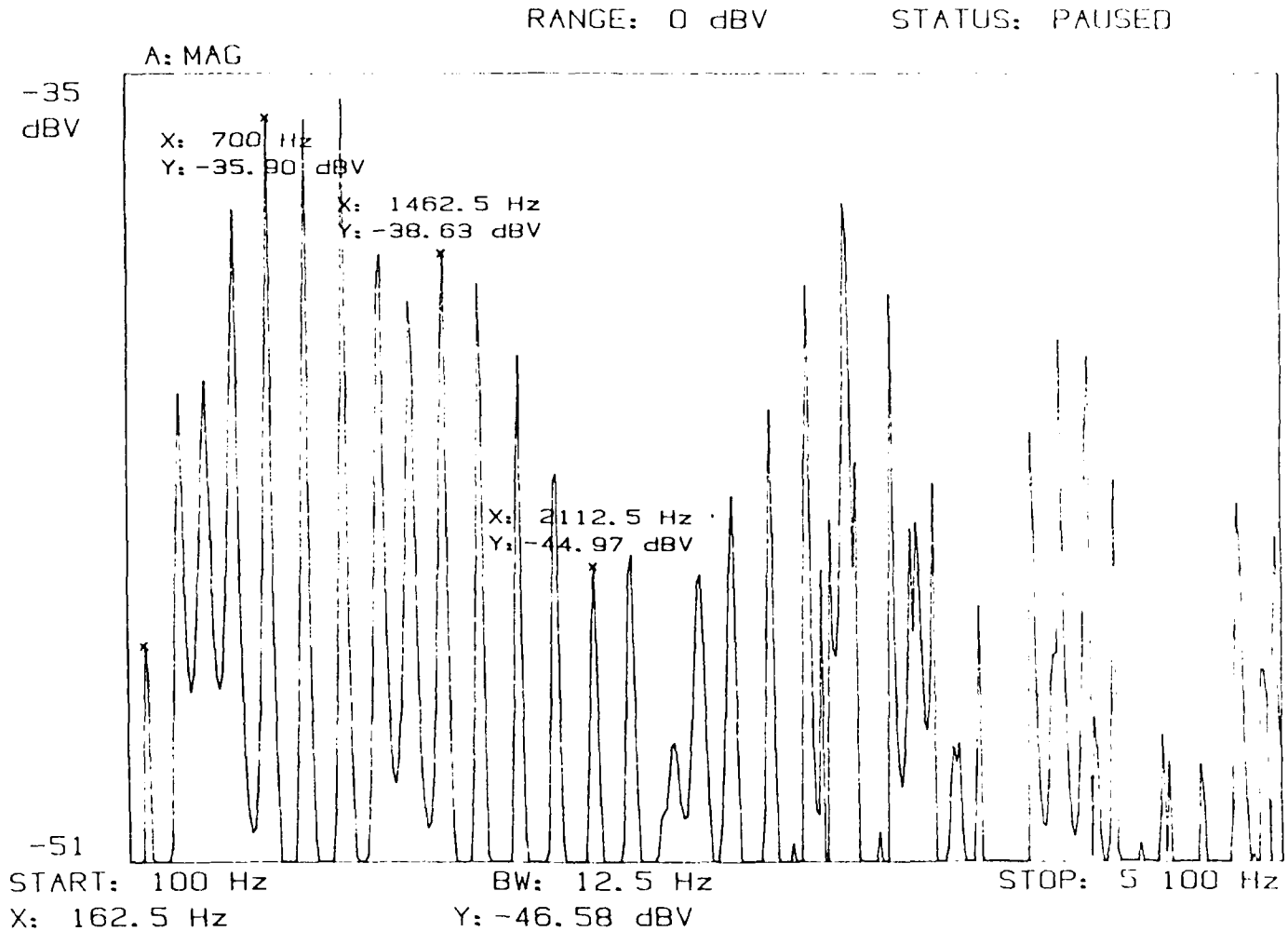

Figure 9 -Natural Resonances of Argon Filled Tube

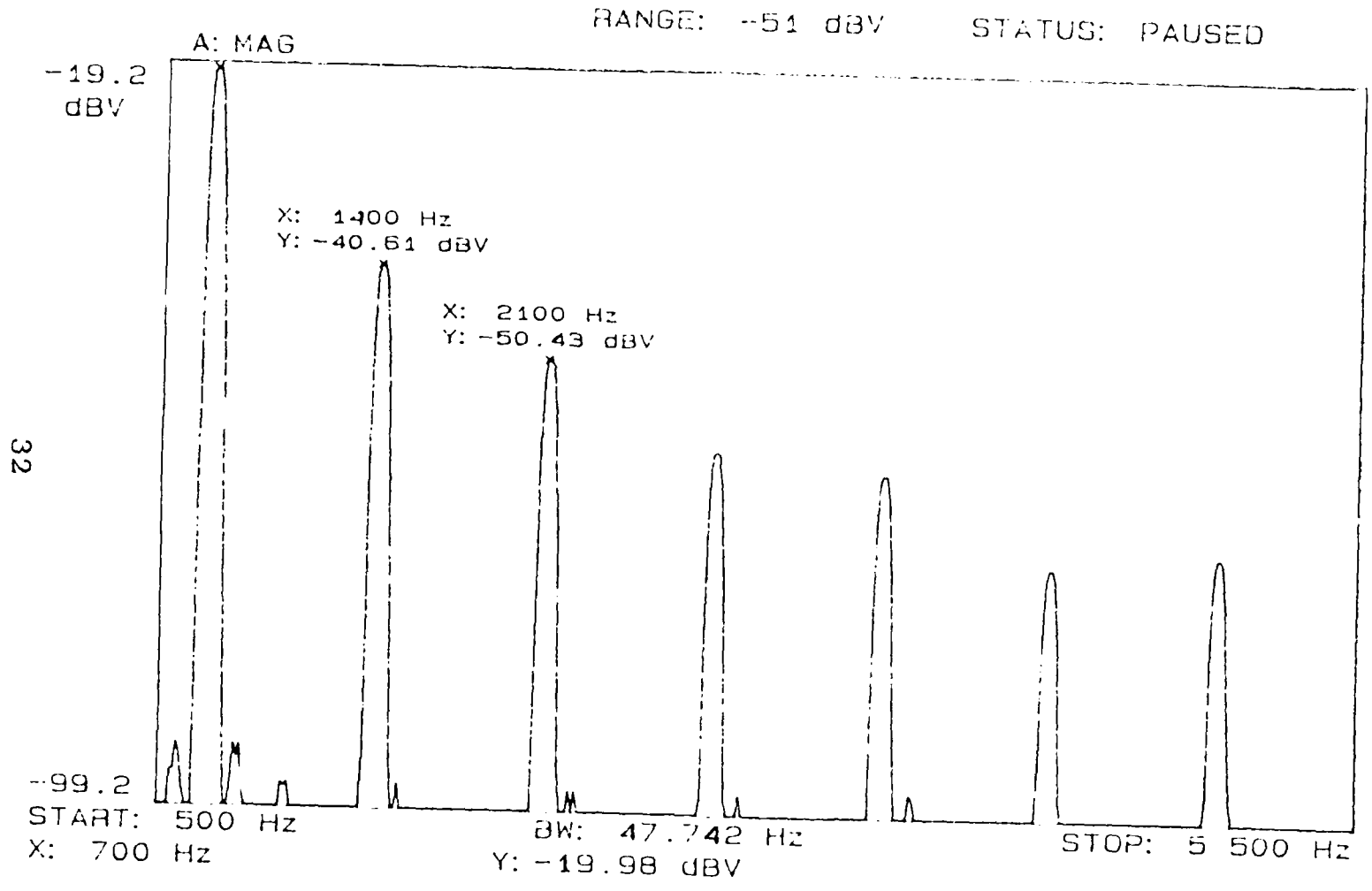

Figure 10 -Harmonics of Argon Filled Tube Driven at 706 Hz
Sound Pressure Level = 162 dB

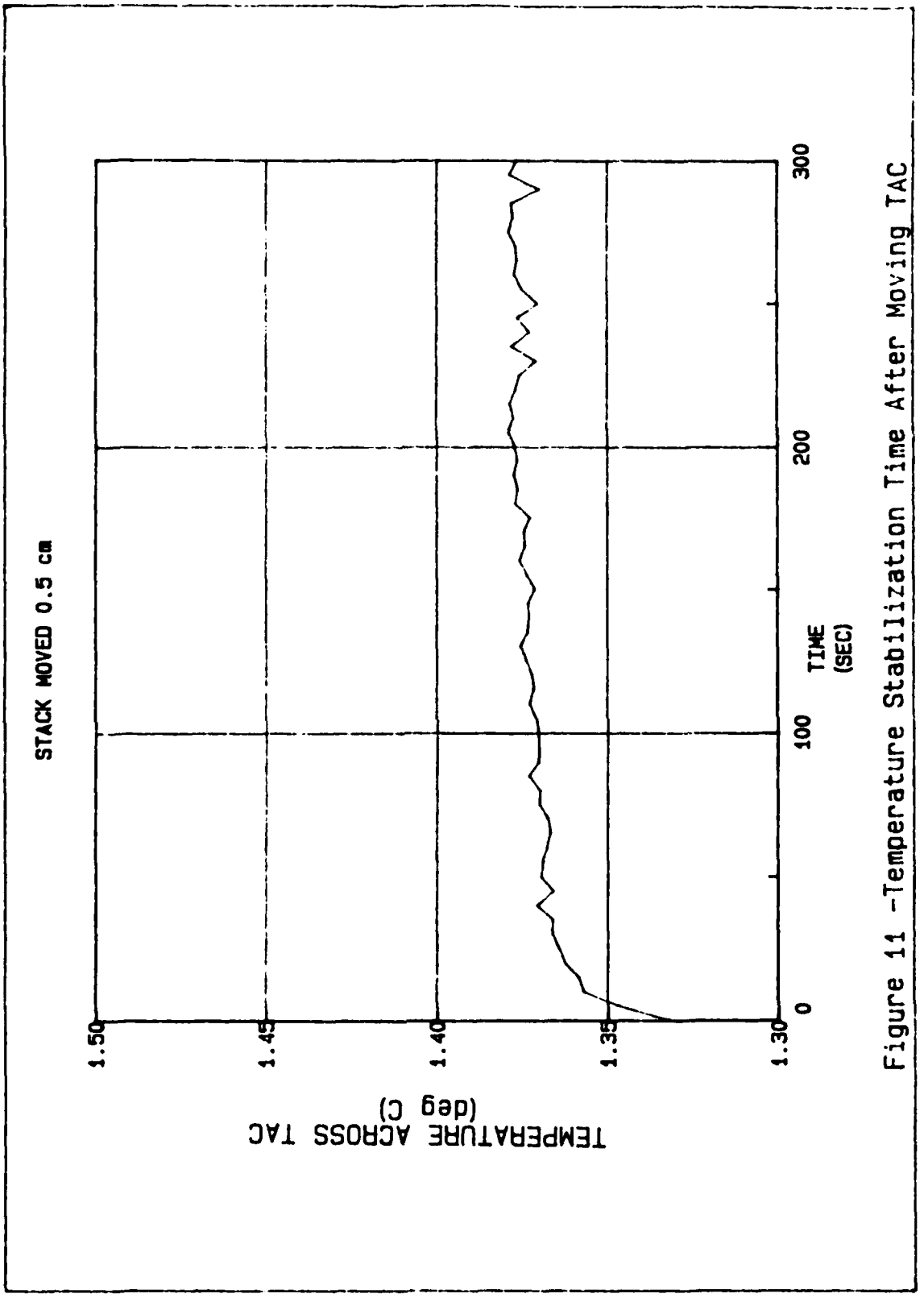

Figure 11 -Temperature Stabilization Time After Moving TAC

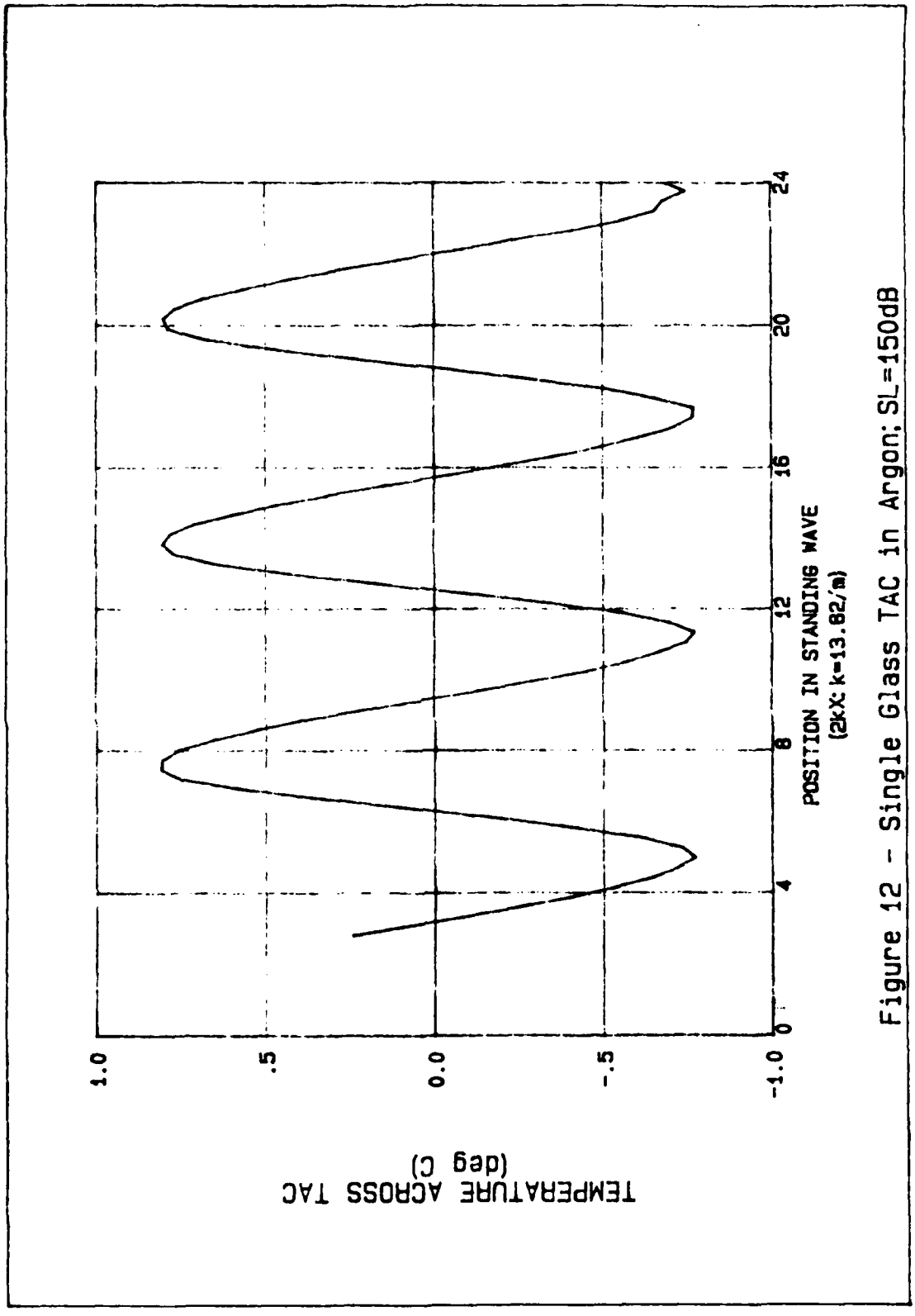

Figure 12 - Single Glass TAC in Argon; SL=150dB

sink" arrangement also limited random voltages caused by temperature variations along the leads, but not at the TAC.

The temperature difference developed across the TAC, as a function of position from the rigid end of the tube, was measured for acoustic pressure levels of 145, 150, and 162 dB re 20 μ Pa (rms). Next, stacks of 3 and 5 plates were constructed by stacking one or two steel plates above and below the measurement TAC at a separation distance of approximately 10 thermal penetration depths. Again, the temperature difference as a function of position was measured at pressure levels 150 and 162 dB. The measurements were then repeated for a separation distance of 36 thermal penetration depths and then for a stack of 3 plates separated by 4 thermal penetration depths.

To ensure that the data were reproducible, the initial data measurements were taken twice. Typical agreement in measured values is depicted in Figure 13. As more data runs were completed, the reproducibility of the data was verified. Therefore, data from later runs were verified by retaking only random data points.

The final measurements in this phase of the study were made in a Helium-filled tube. The new resonances of the tube were found (see Figure 14) and the driving frequency 2120 Hz was chosen to maintain the wavelength to TAC length ratio used in the Argon-filled tube. In this portion of the experiment, a stack of 3 plates separated by 6 thermal penetration depths was used for pressure levels of 150 and 162 dB.

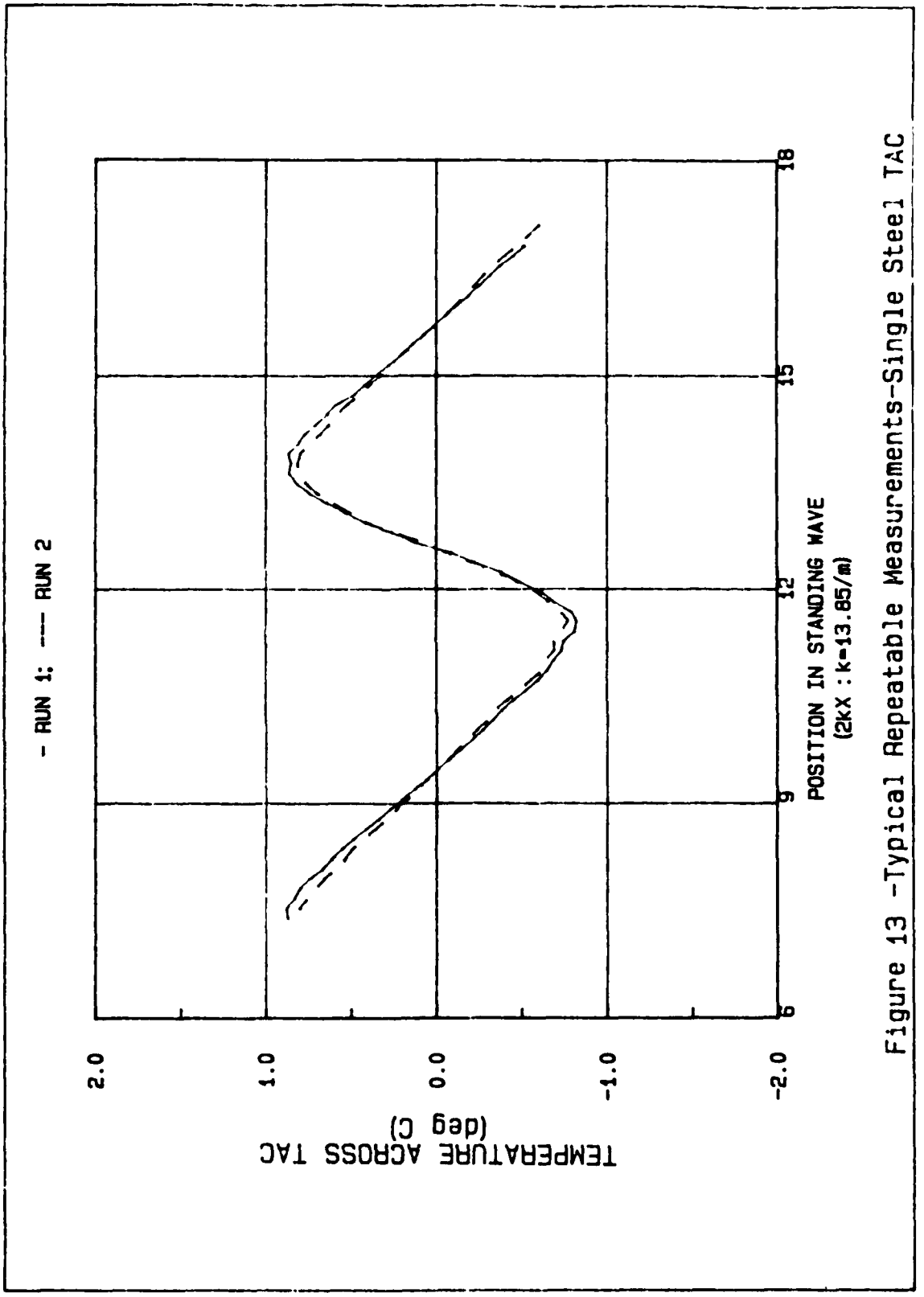

Figure 13 -Typical Repeatable Measurements-Single Steel TAC

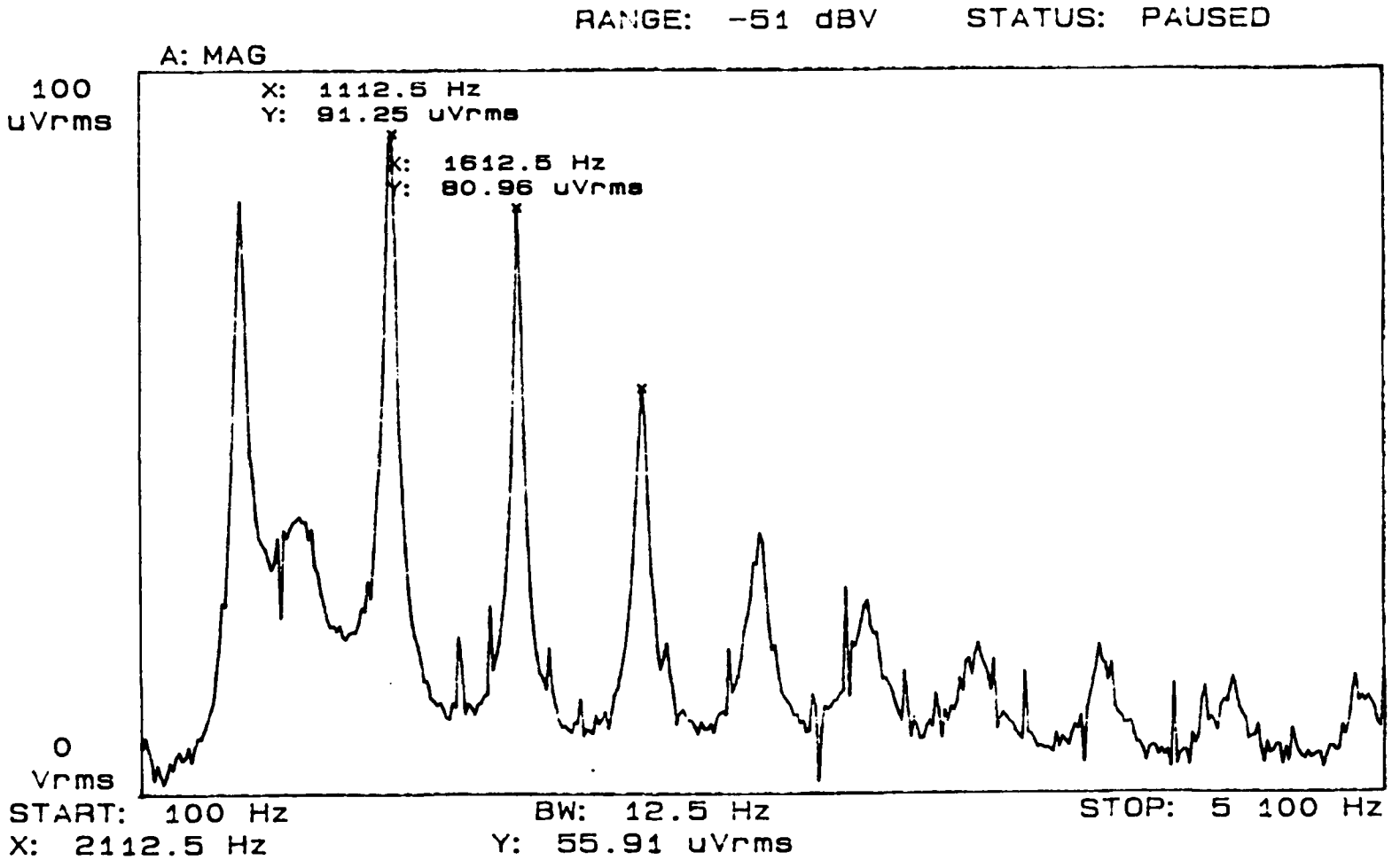

Figure 14 -Natural Resonances in Helium Filled Tube

B. DIAMETRICAL MAPPING

Before probing the tube diameter, the results of phase 1 were perused to determine a position within the tube where a reasonable temperature difference was established at all pressure levels studied. This position was 41.5 cm from the endplate, where $2kx \approx 11.5$. The tube was then cut at this position, the apparatus shown in Figure 15 inserted, and the tube sections rejoined. Again, the tube was filled with Argon and the resonances were found (see Figure 16). The resonance frequency closest to the driving frequency used in the first experiment was chosen as the driving frequency for this experiment. For acoustic pressure levels of 150 and 162 dB, the temperature difference across the single TAC was measured as a function of position along the diameter of the tube. Then the same measurement was made for the center plate of a stack of 3 plates separated by 10 thermal penetration depths.

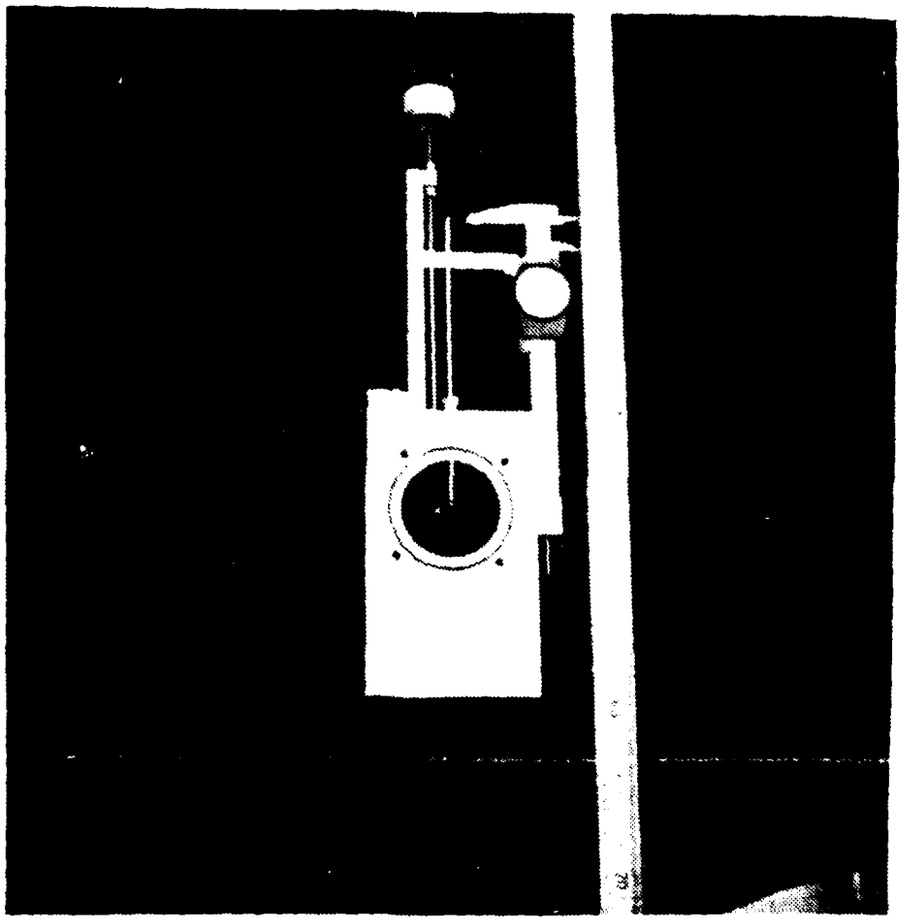

Figure 15 -Insert to Measure Diametric Temperature Gradient Variations

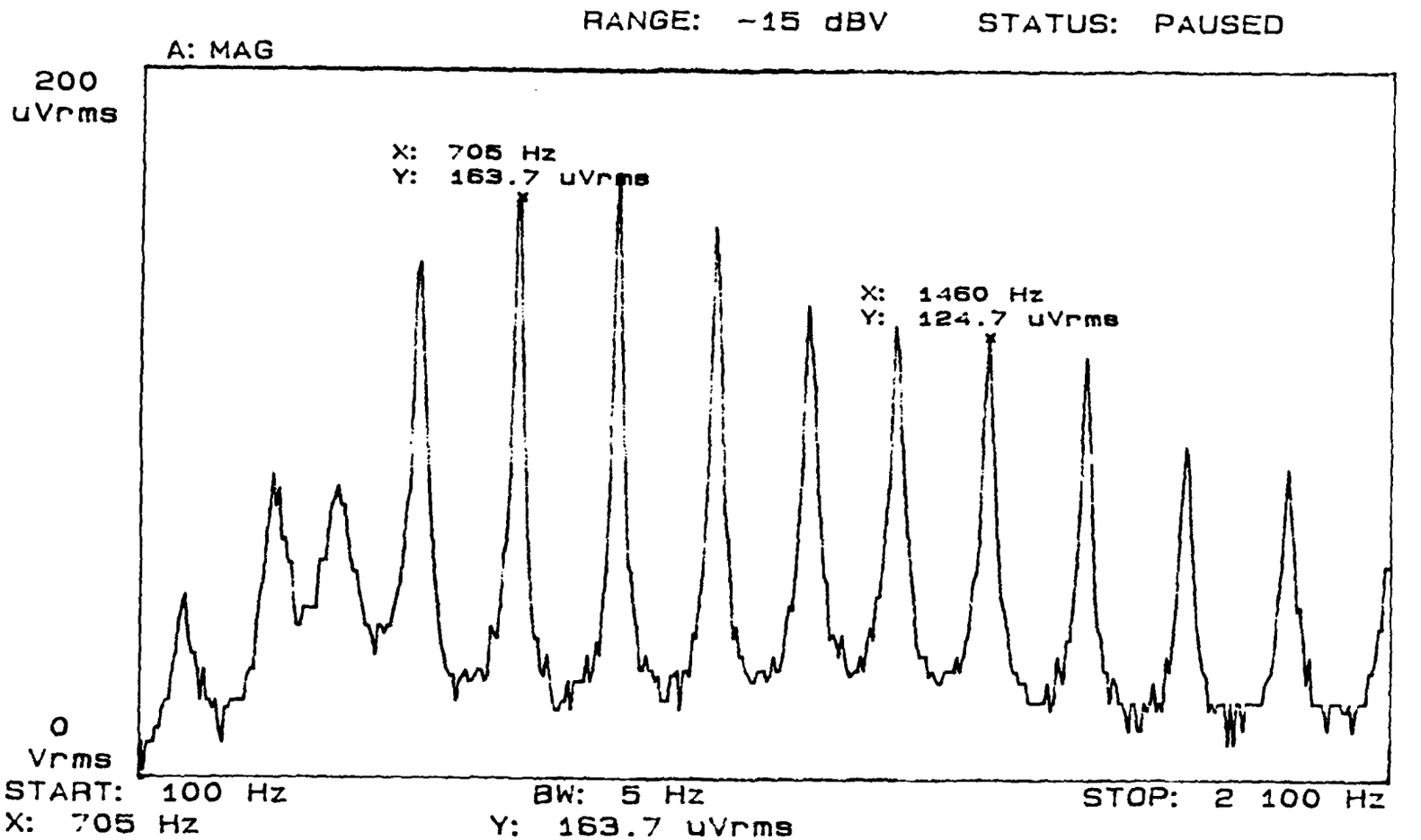

Figure 16-Natural Resonances of Argon Filled Tube with Insert

IV. RESULTS

A. LONGITUDINAL MAPPING

As previously described, a TAC constructed of a single glass plate was used in a trial measurement. As can be seen in Figure 17, at an acoustic amplitude near 150 dB re 20μPa (rms), the measured temperature difference and acoustic amplitude have the predicted relationship (i.e., the temperature difference varies approximately sinusoidally with zero crossings corresponding to acoustic pressure maxima and minima).

The temperature difference across the single stainless steel TAC was measured as a function of tube position and pressure amplitudes. The results are shown in Figures 18 through 20. In these figures, the solid line represents the experimental values; the dashed and dotted lines represent Theory and Mod Theory, respectively. At acoustic amplitudes of 145 and 150 dB re 20μPa (rms), the measured temperature difference falls between the values predicted by both Theory and Mod Theory calculation methods (Figure 18 and 19). At the higher level of 162 dB, the peak temperature difference is at least 2° C (or approximately 50 percent) lower than that predicted by either theoretical method (Figure 20). However, there is still good agreement near the pressure antinode ($2kx \approx 12.7$). Additionally, skewing of the data toward the pressure antinodes is evident, yet not predicted.

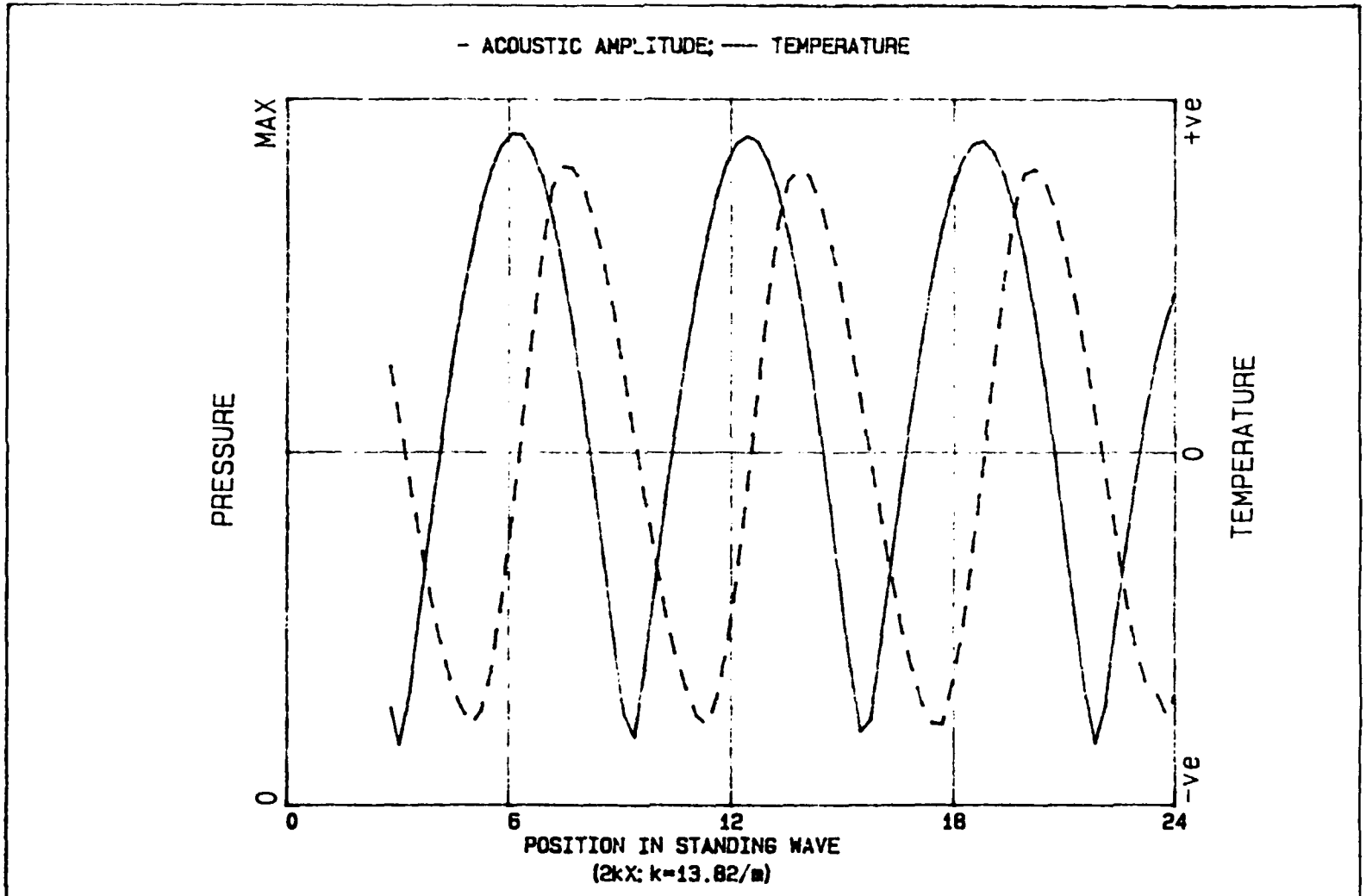

Figure 17-Acoustic Amplitude and Glass TAC Temperature Difference

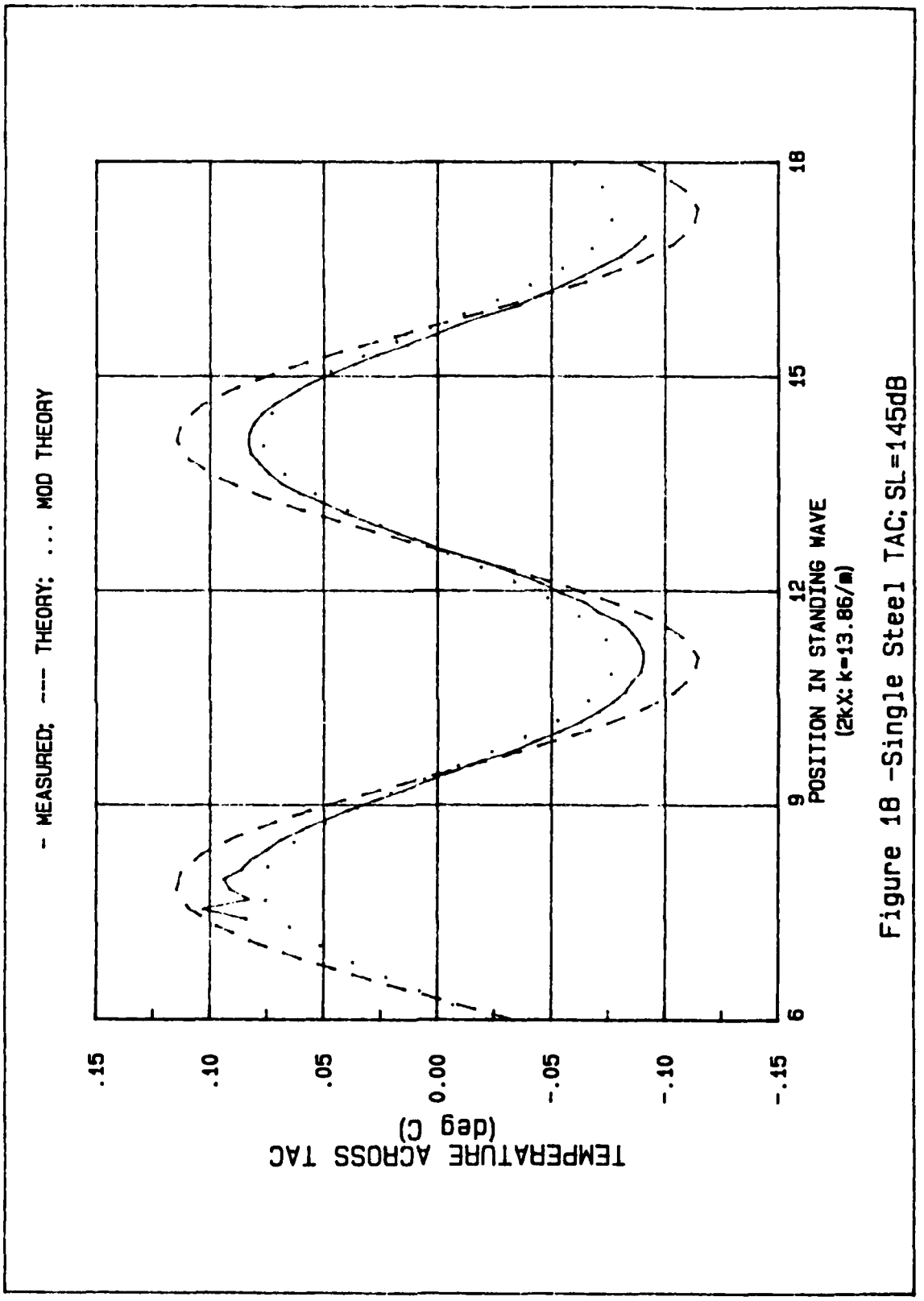

Figure 18 -Single Steel TAC; SL=145dB

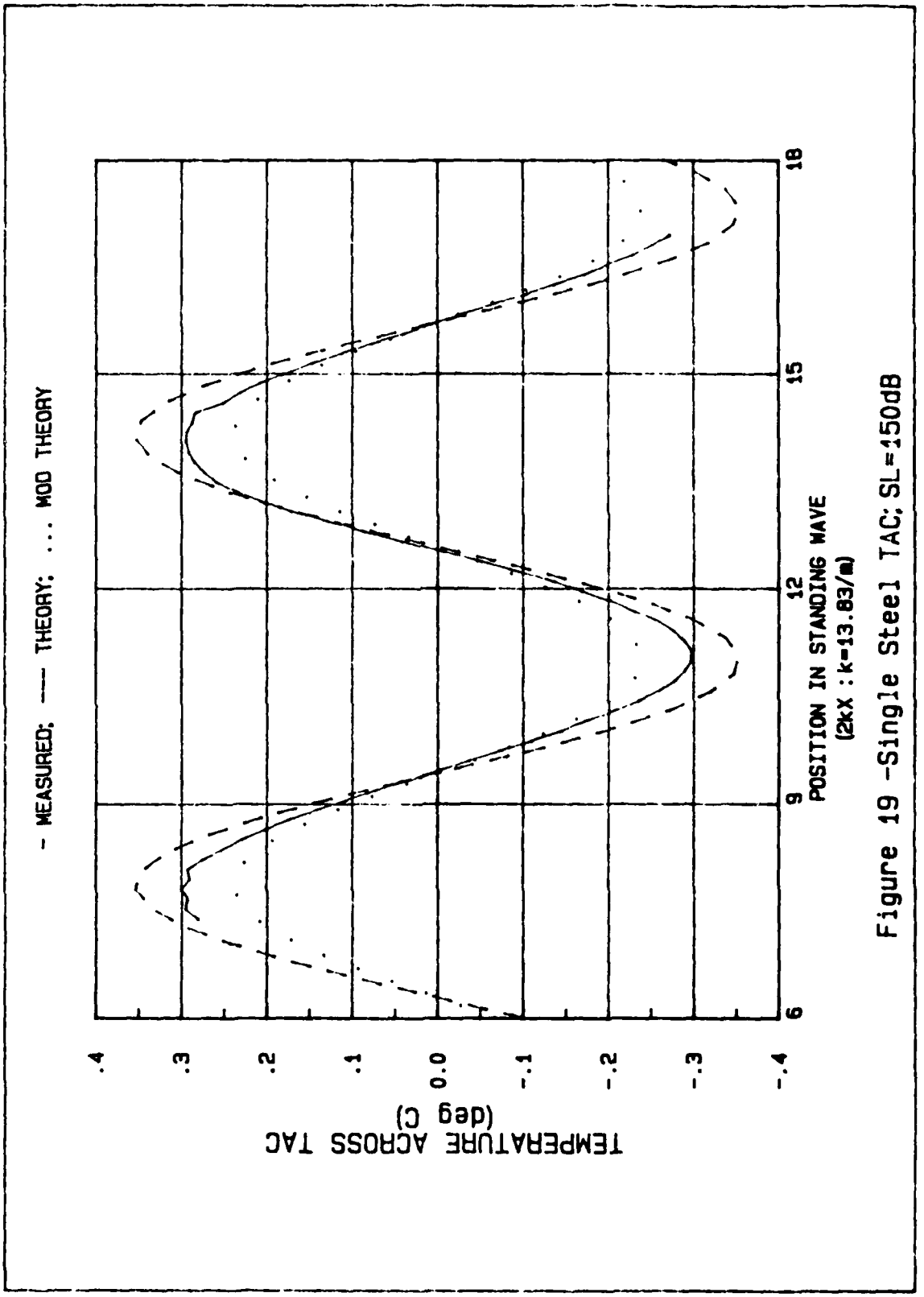

Figure 19 -Single Steel TAC; SL=150dB

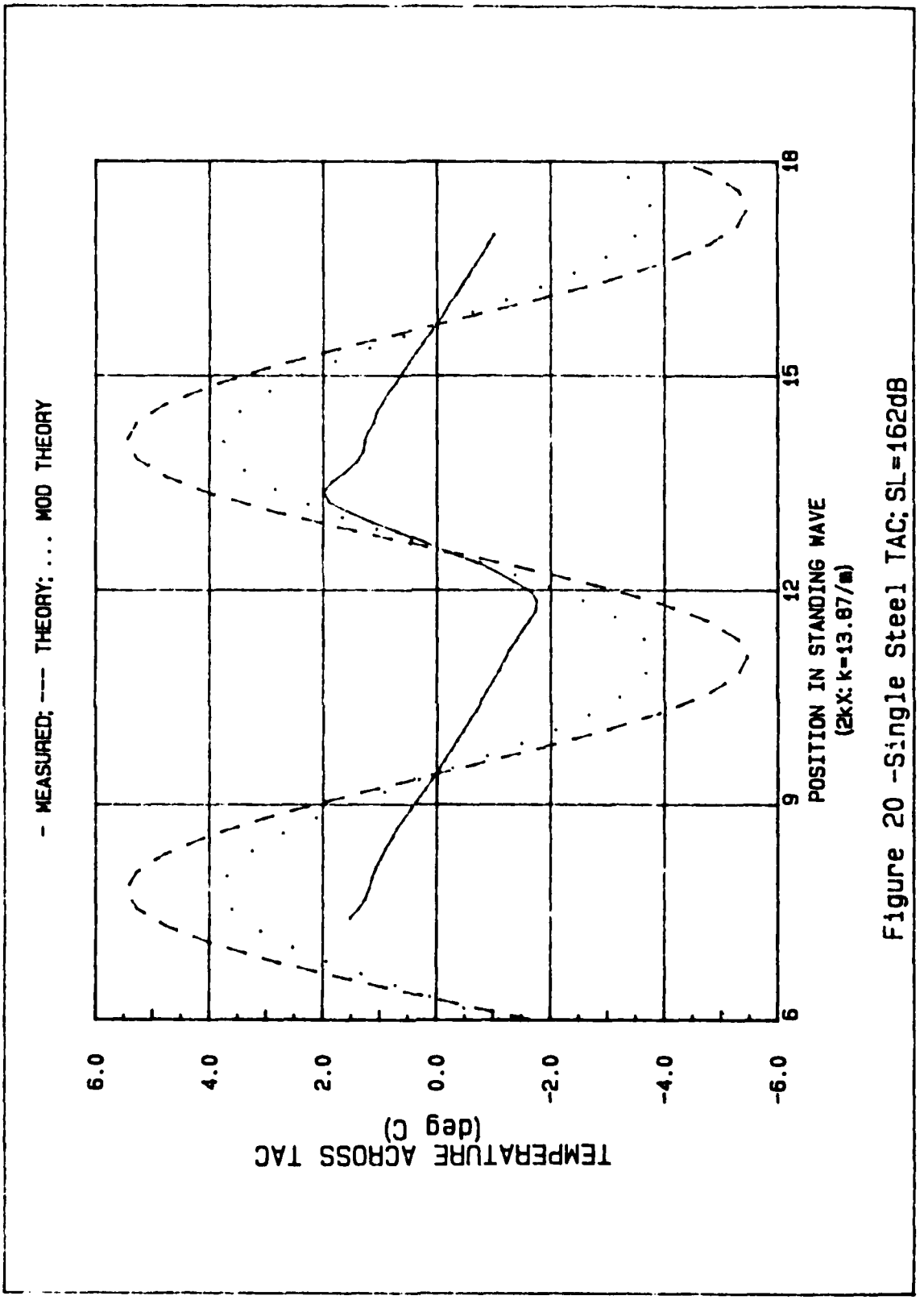

Figure 20 -Single Steel TAC; SL=162dB

When stacks of 3 and 5 plates, with a plate separation of 36 thermal penetration depths, are used at an acoustic pressure of 150 dB, there again is close agreement between measured and predicted data (Figure 21). The agreement between the observed temperature differences for a 3 or 5 plate stack is within experimental fluctuation observed on repeat data runs, as discussed earlier (Figure 13). At the higher sound level of 162 dB, a large discrepancy, 2° C (about 50 percent), between measured and predicted peak temperature differences is observed (Figure 22), although the agreement near the pressure antinode is still good. Again, the 3 and 5 plate stacks produce comparable results.

When measurements are made using stacks with plate separations of 10 thermal penetration depths, there is again agreement between measured and predicted data at the low acoustic amplitude (Figure 23) and disagreement at the high amplitude (Figure 24). In this case, the magnitude of the disagreement is smaller (only 1° C or about 30 percent) than the predicted peak. This disagreement is not as much as that for a single plate or for a stack with 36 penetration depth spacing. Additionally, there again appears to be a strong similarity between the results for the 3 plate and 5 plate stacks.

With a stack consisting of 3 plates, separated by 4 thermal penetration depths, again there is good agreement between observed and theoretically calculated temperature differences at a low level of acoustic pressure (Figure 25). Figure 26 shows the now-familiar discrepancy at the higher driving amplitude, but it has increased back to

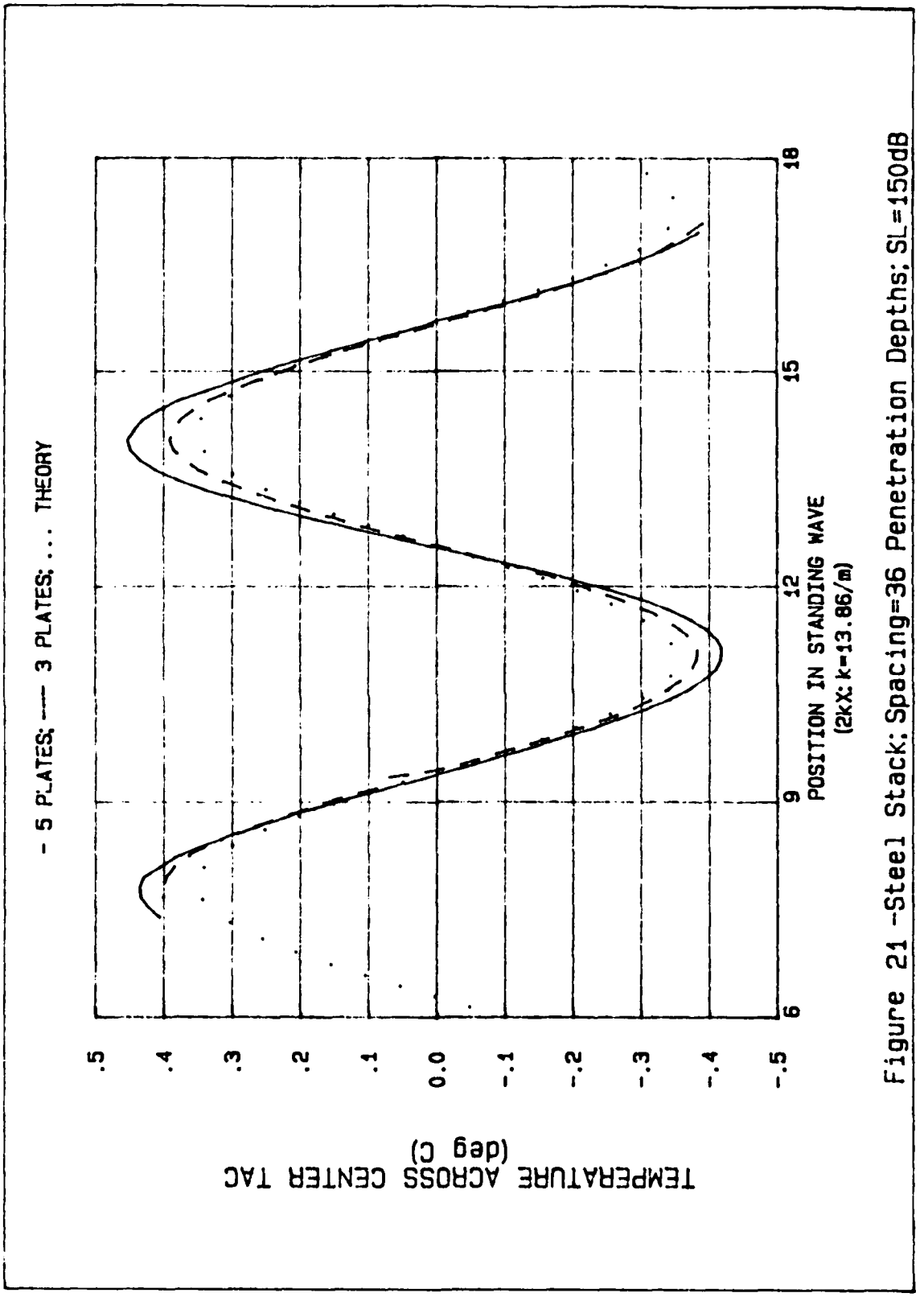

Figure 21 -Steel Stack; Spacing=36 Penetration Depths; SL=150dB

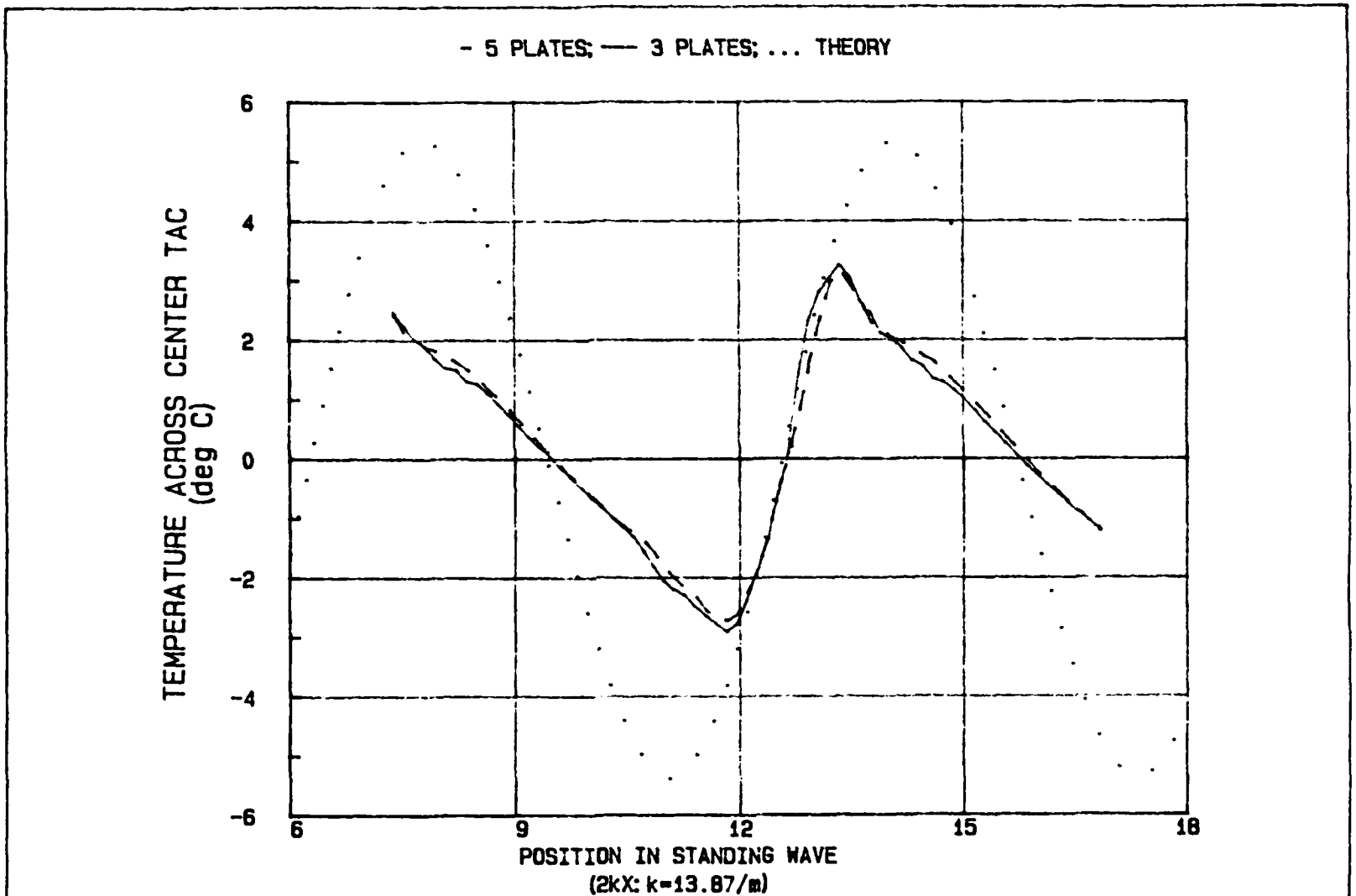

Figure 22 -Steel Stack; Spacing=36 Penetration Depths; SL=162dB

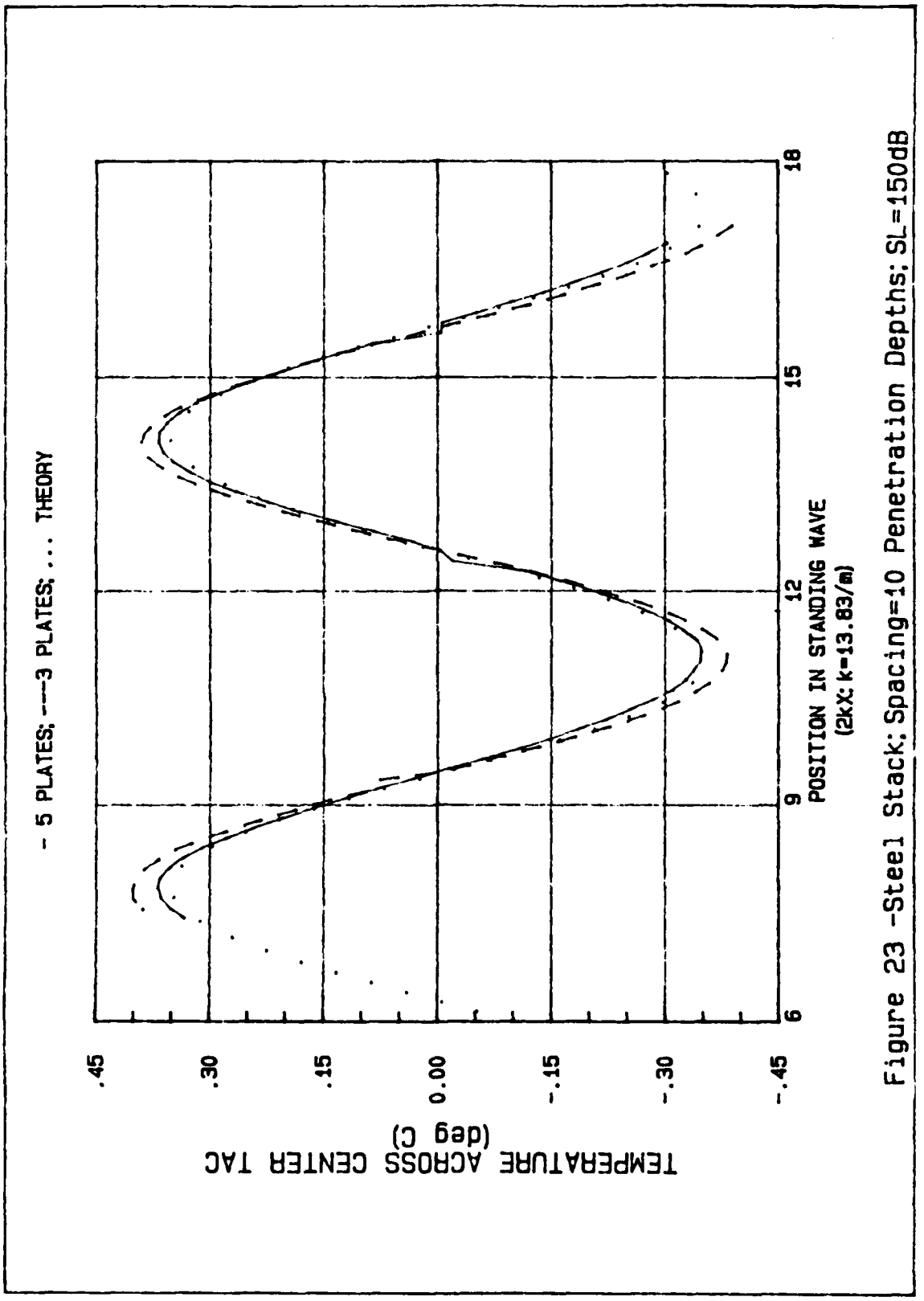

Figure 23 -Steel Stack; Spacing=10 Penetration Depths; SL=150dB

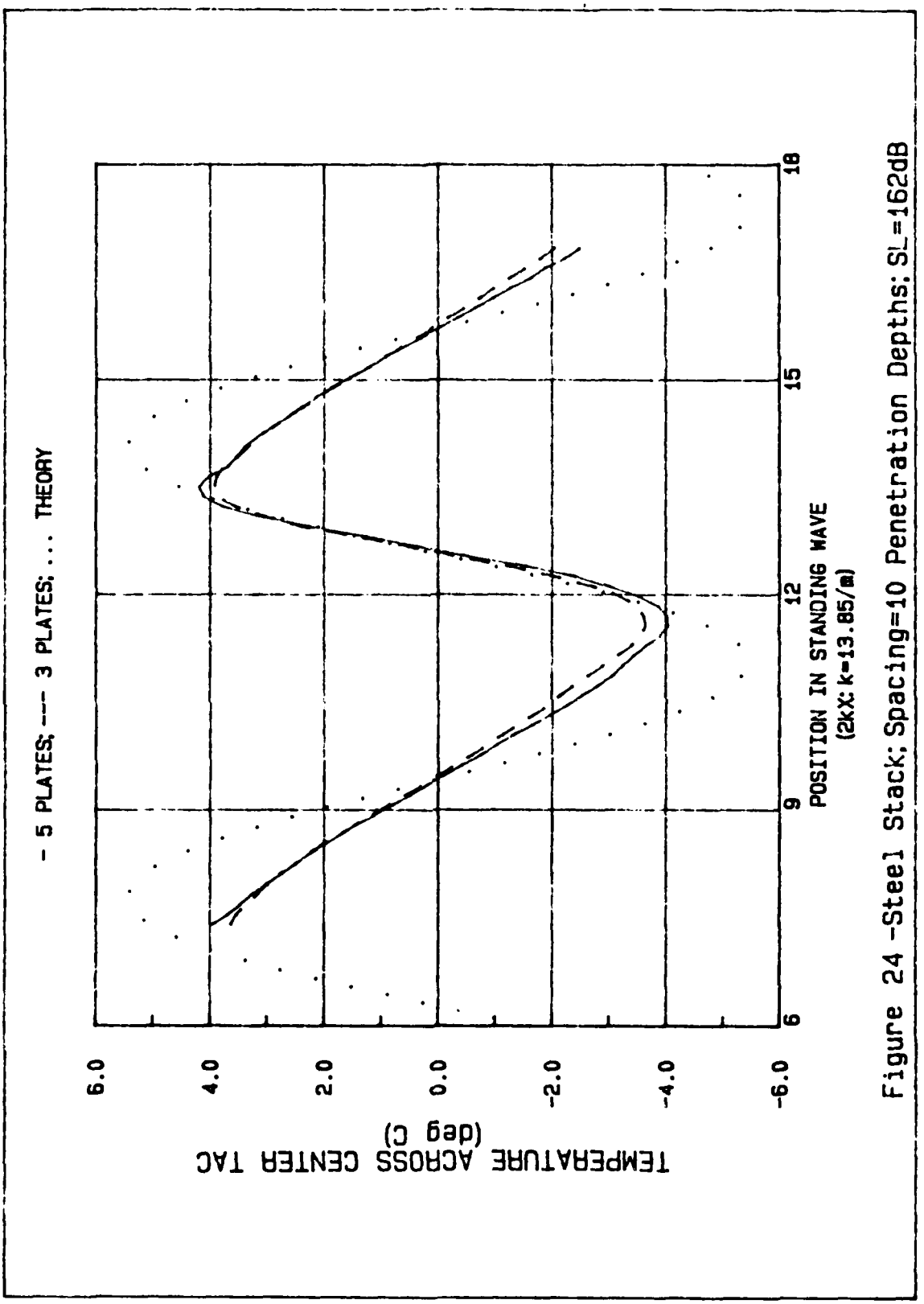

Figure 24 -Steel Stack; Spacing=10 Penetration Depths; SL=162dB

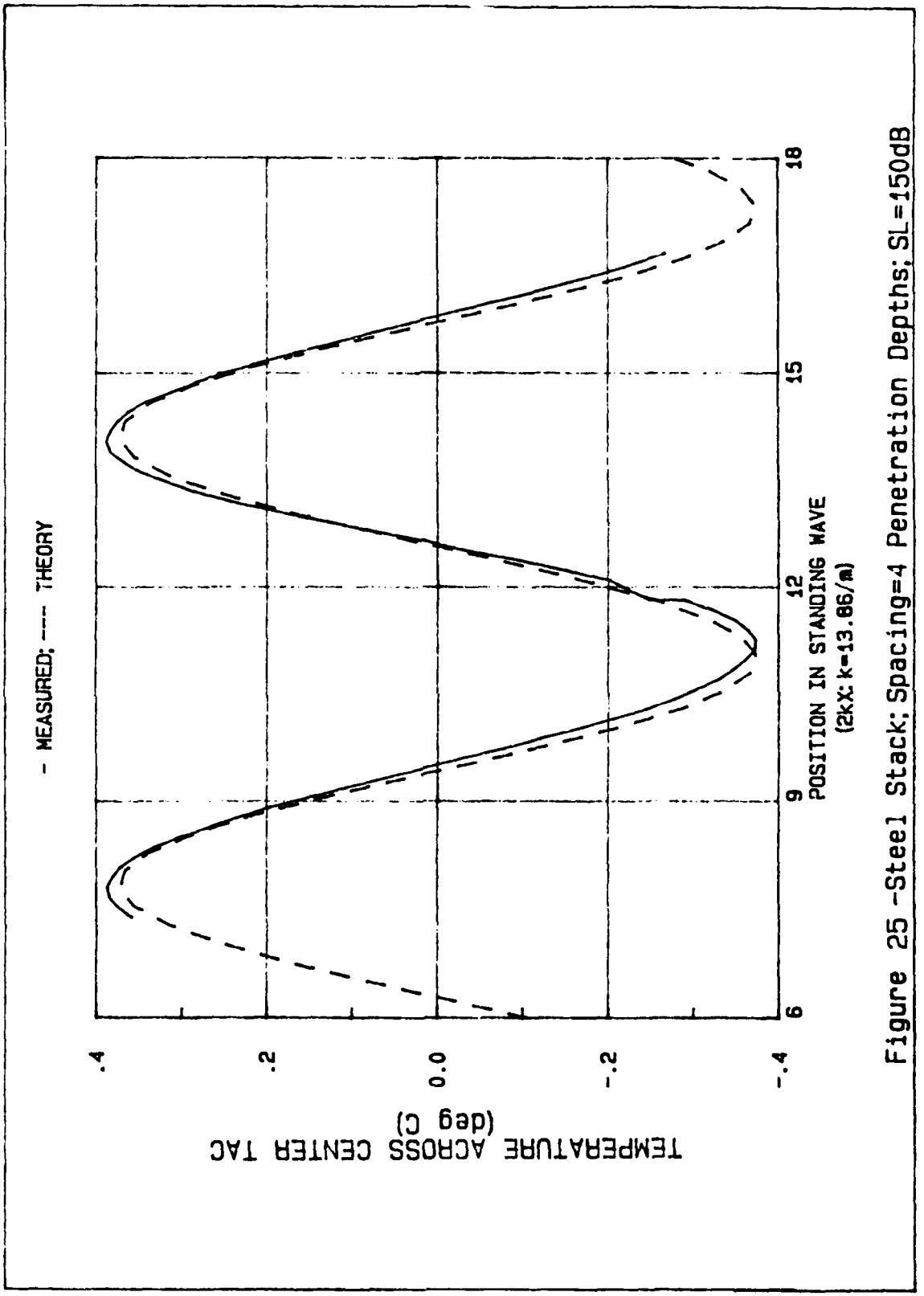

Figure 25 -Steel Stack; Spacing=4 Penetration Depths; SL=150dB

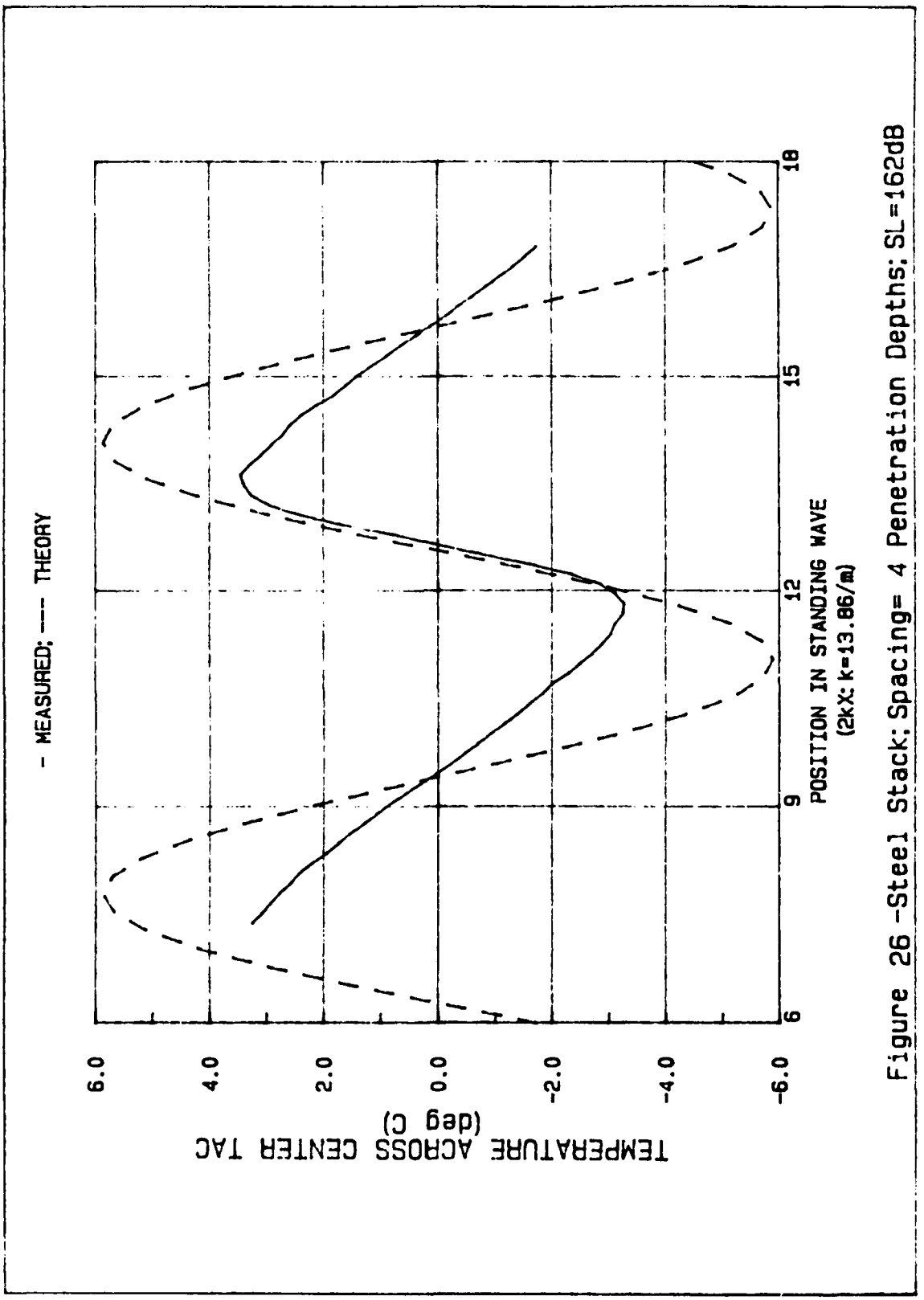

Figure 26 -Steel Stack; Spacing= 4 Penetration Depths; SL=162dB

approximately 2° C (about 50 percent). The noticeable skewing is again present, with good agreement near the pressure antinode.

Finally, this same TAC was used in a Helium-filled tube with a plate separation of 6 thermal penetration depths. While the measured data are approximately 1° C (50 percent) lower than predicted at the 150 dB level, the shape of the resulting curve is as predicted (Figure 27). However, at the 162 dB level, the discrepancy increases to approximately 16° C (about 70 percent) lower than the maximum predicted. Also, as with the Argon data, the agreement is best near the pressure antinode. Furthermore, the observed skewing is much more pronounced than predicted (Figure 28). In this figure, the encircled jump in the data is the result of a blown fuse in the driver circuit which had to be replaced before data acquisition could continue.

B. DIAMETRICAL MAPPING

In this experiment, the diameter of the tube was probed with two TAC structures. First, using a single steel TAC, the temperature difference variations across the diameter were measured for acoustic amplitudes of 150 and 162 dB (Figures 29 and 30). At the lower level, the temperature difference magnitude increases, albeit less than 0.01° C (3 percent), as the TAC was moved across the diameter. At the 162 dB level, the difference magnitude increases about 0.15° C (10 percent) across the diameter. The probe construction prohibited measurement within 0.9 cm of the tube wall. The 3.11 cm distance corresponds to the tube center.

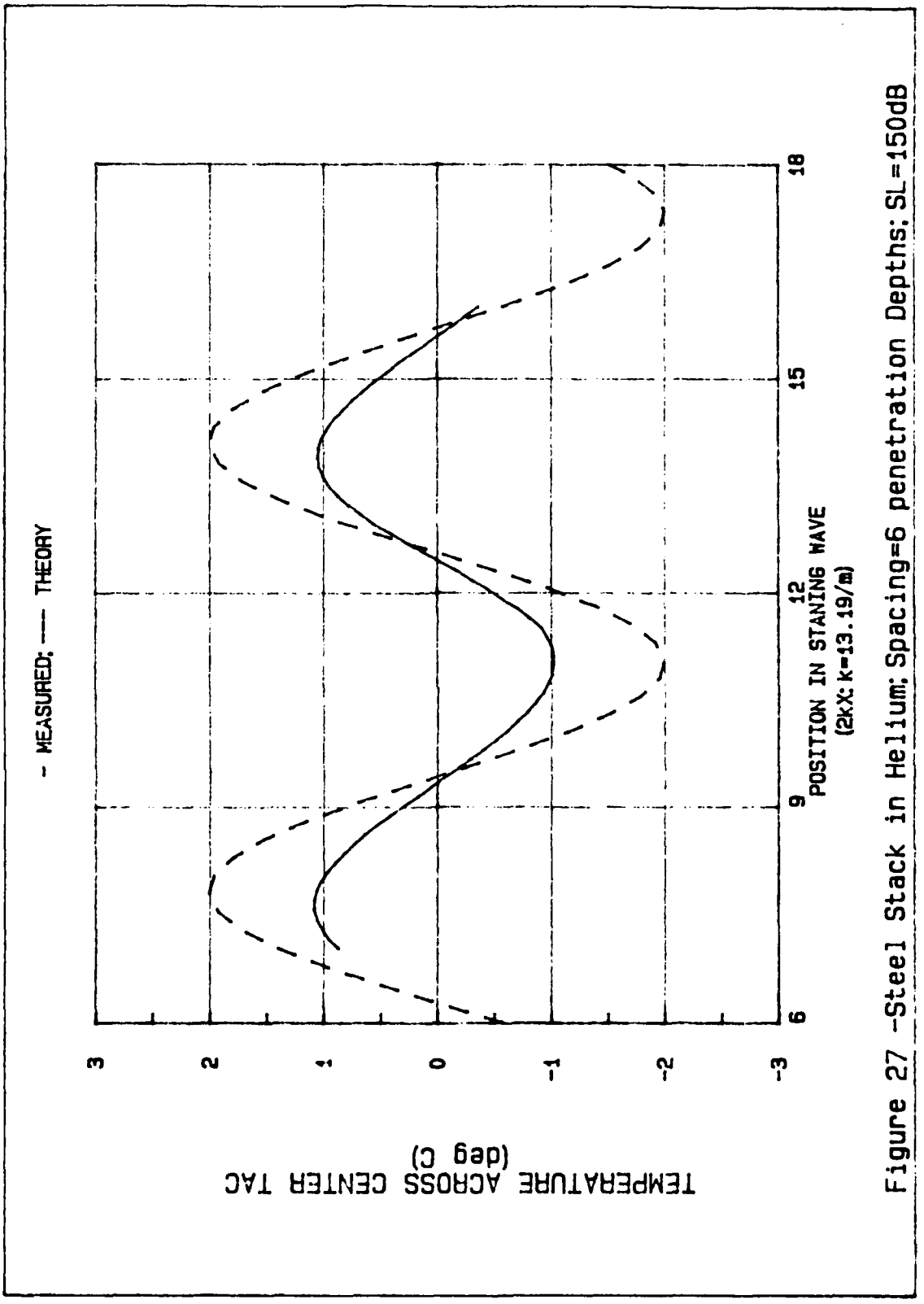

Figure 27 -Steel Stack in Helium; Spacing=6 penetration Depths; SL=150dB

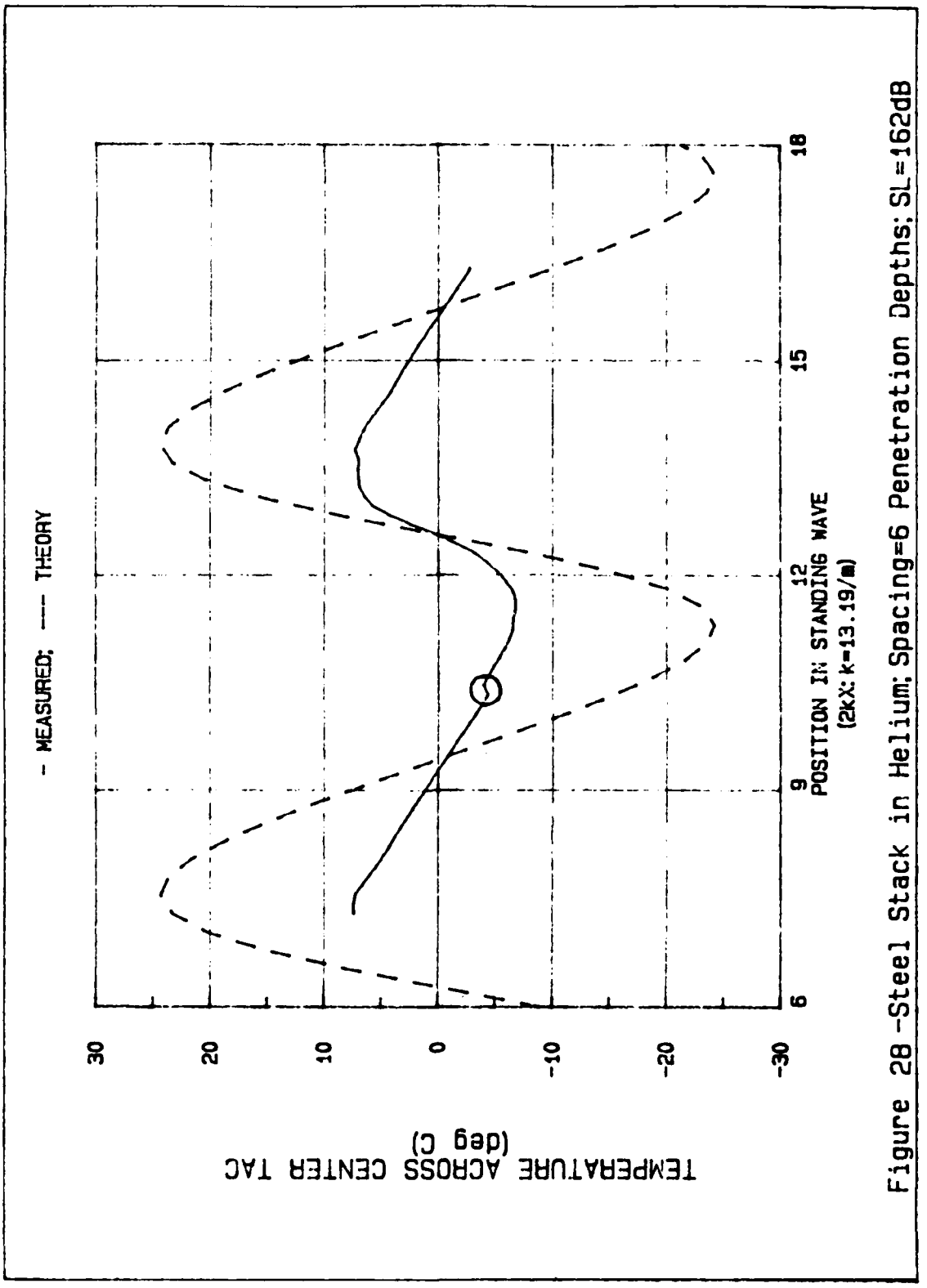

Figure 28 -Steel Stack in Helium; Spacing=6 Penetration Depths; SL=162dB

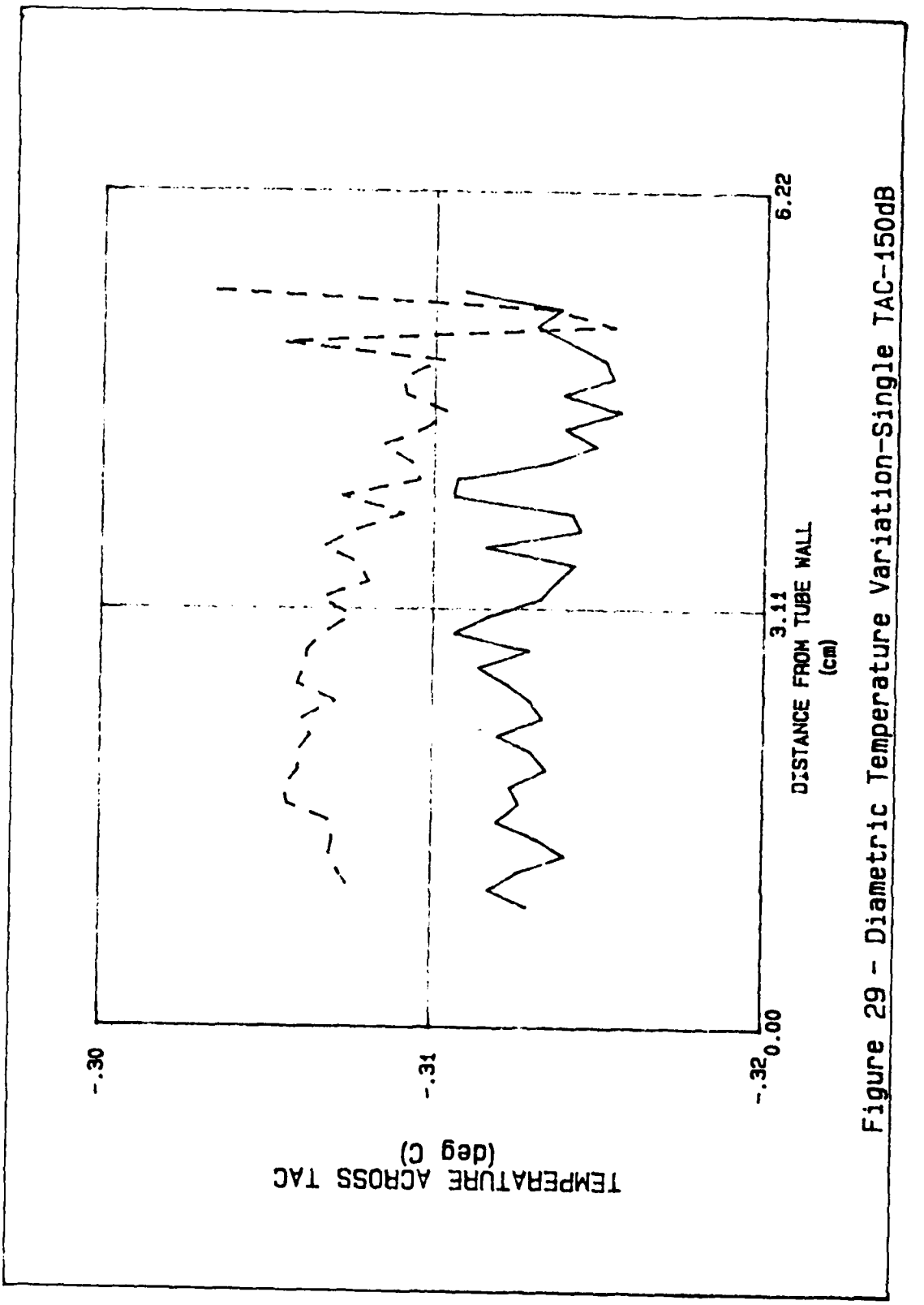

Figure 29 - Diametric Temperature Variation-Single TAC-150dB

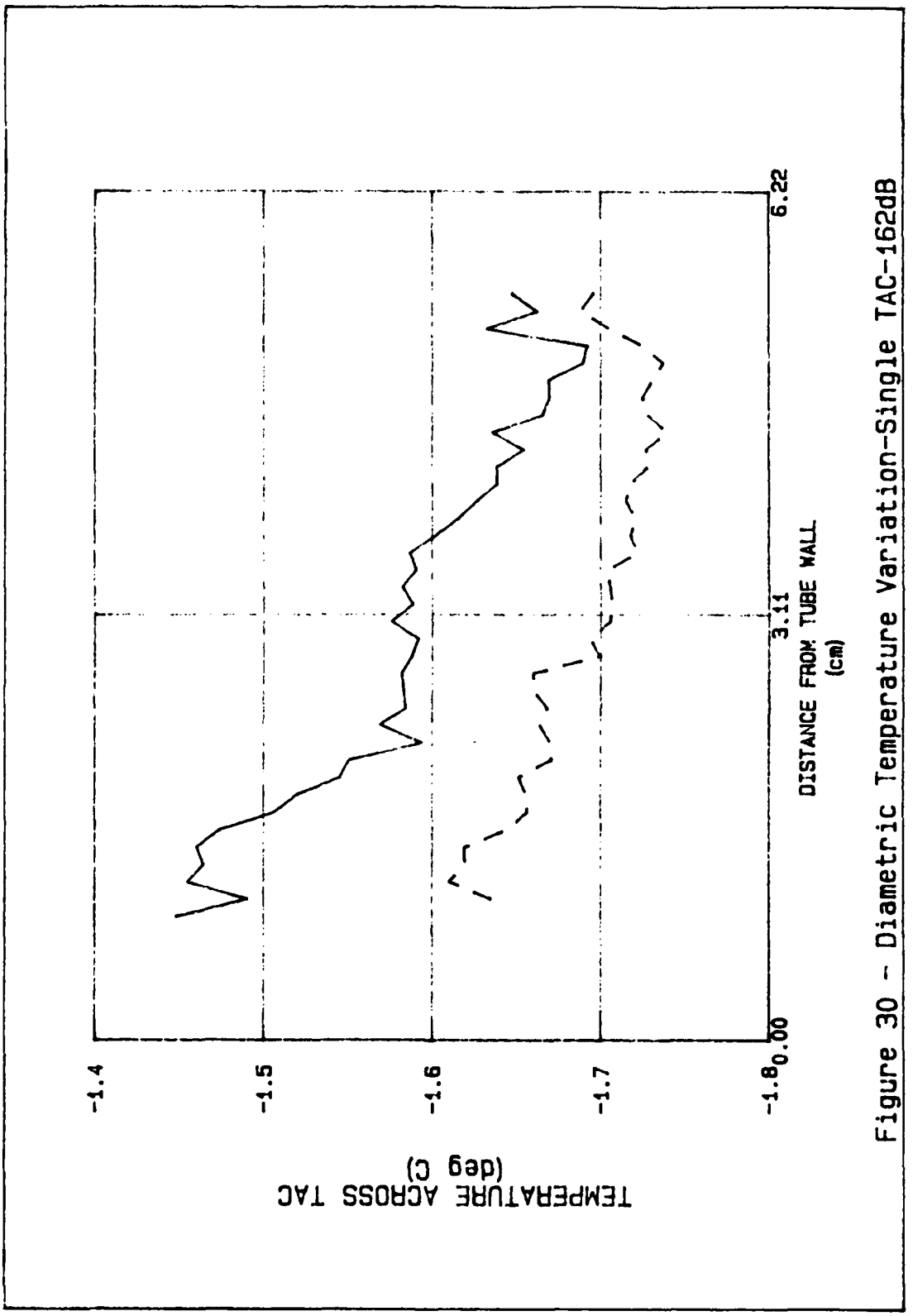

Figure 30 - Diametric Temperature Variation-Single TAC-162dB

Next, the measurements were repeated using a 3 plate stack with a plate separation of 10 thermal penetration depths (Figures 31 and 32). At 150 dB, there is a slight decrease in magnitude, 0.05° C (about 10 percent), across the diameter. There was an interesting result observed at 162 dB: The temperature difference went through a maximum near the tube center, with a temperature swing of 0.2° C (5 percent).

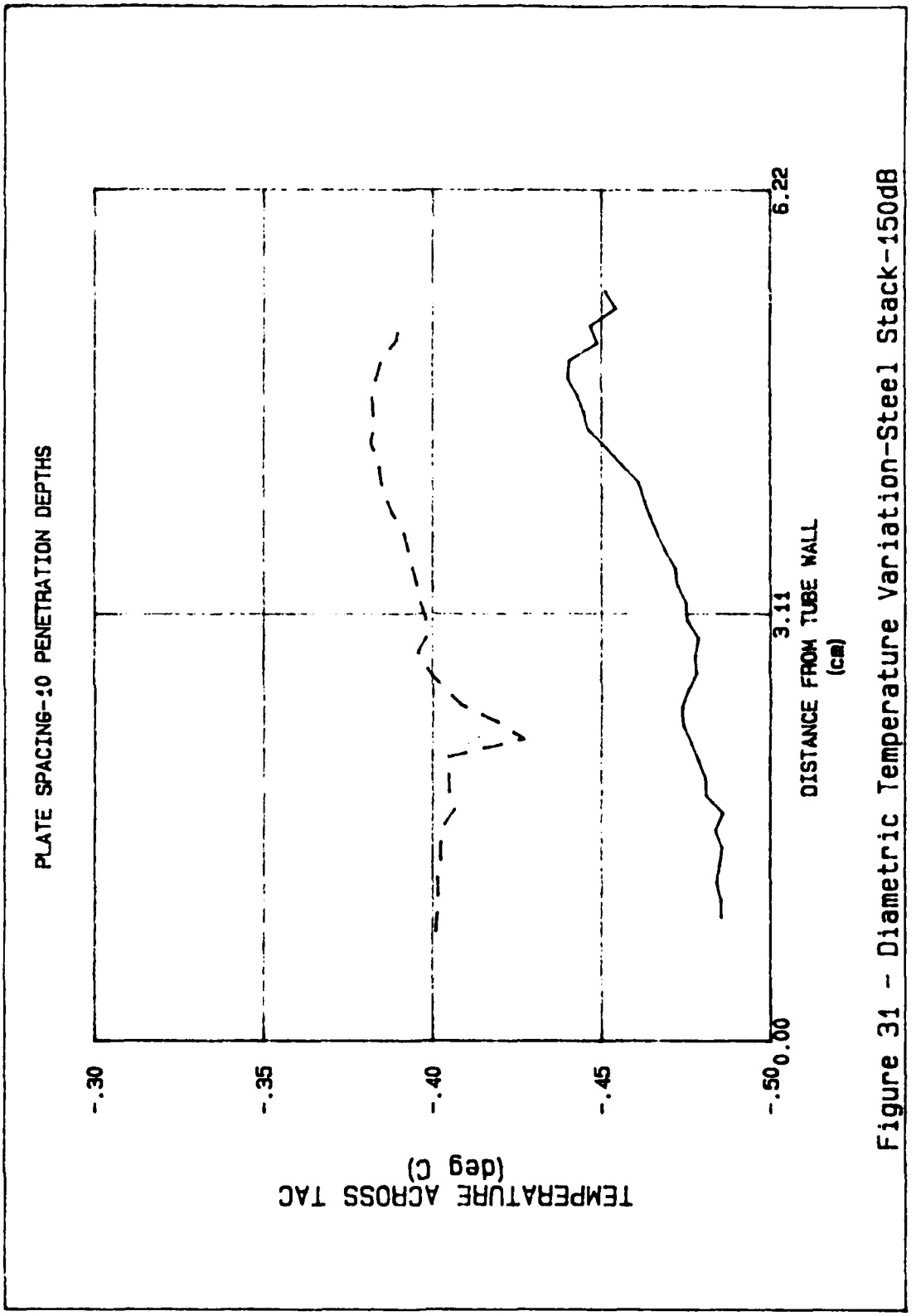

Figure 31 - Diametric Temperature Variation-Steel Stack-150dB

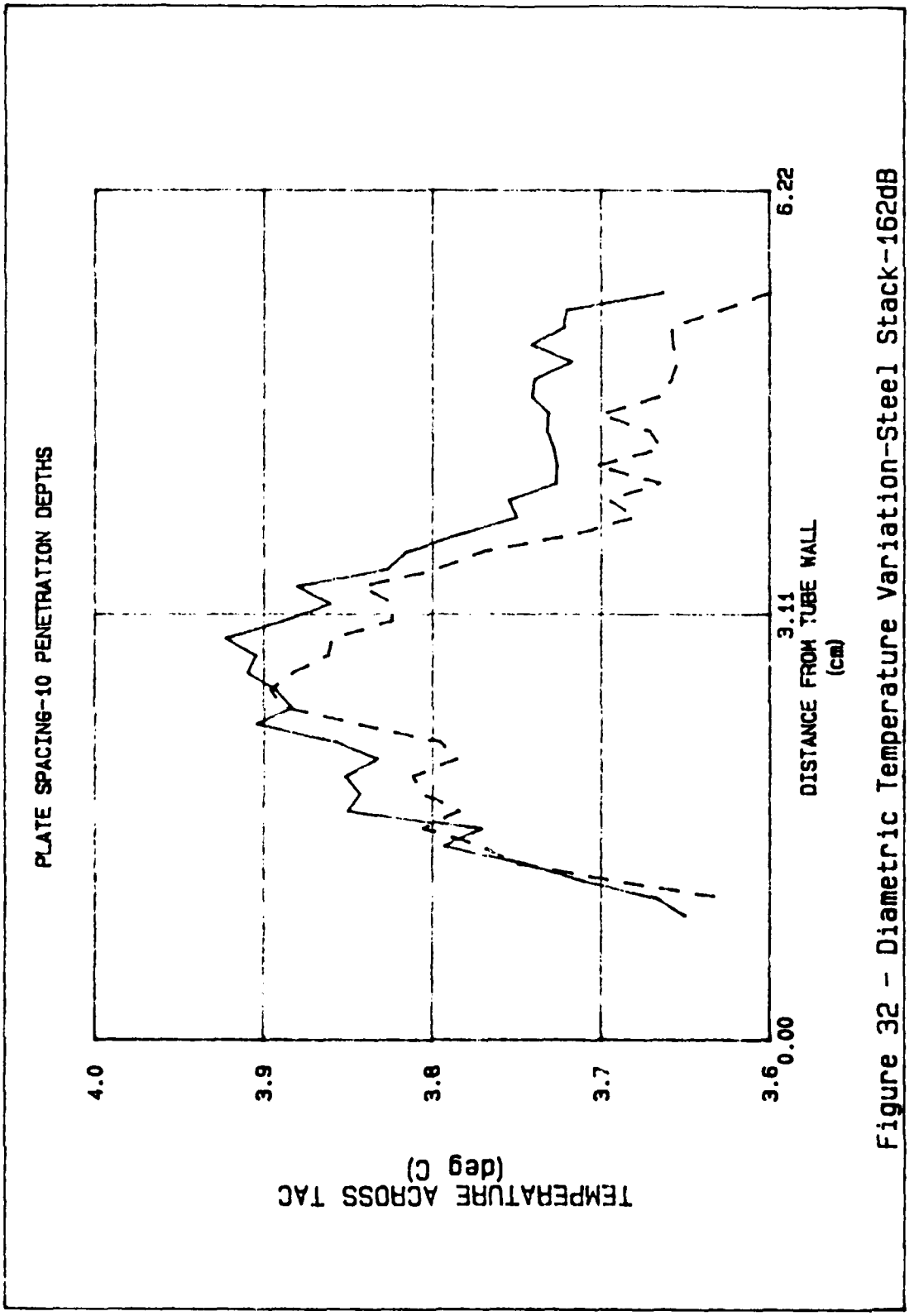

Figure 32 - Diametric Temperature Variation-Steel Stack-162dB

V. DISCUSSION

The modifications made to Wheatley's theory allow for consideration of the return path through the gas, which Wheatley considered insignificant for a steel plate TAC. For a single plate TAC at low amplitude, Theory and Mod Theory are both in good agreement with the measured data (Figures 18 and 19). It was stated in Chapter II that the Theory and Mod Theory represented lower and upper limits to the temperature difference across the TAC. This prediction was confirmed at low pressure amplitudes where the experimental data falls between the two predictions (Figures 18 and 19). At the higher acoustic amplitude, neither theory can account for the lower temperature gradient observed across the TAC (Figure 20).

It was believed that by studying stacks of plates the cause of this discrepancy could be found. For stacks of 3 and 5 plates at various separations, the measured data at low acoustic amplitudes compares favorably with theory (Figures 21, 23, and 25). This agreement is observed no matter the spacing or the number of plates. Even with a different gas, there is reasonable agreement (Figure 27). However, at the higher acoustic amplitude, the magnitude of the temperature difference is noticeably smaller than predicted, regardless of the separation, the number of plates, or the gas in the tube (Figures 22, 24, 26, and 28). Additionally, the skewing phenomenon is observed. It is, therefore, evident that the inclusion of return path through the gas in

the theory is not sufficient to account for the discrepancies observed. Evidently, at higher amplitudes some other processes are causing the discrepancies.

It is interesting to note the effect that variations in plate separation have on the experimental results. As the plate separations are reduced from 3 cm, i.e., a single plate, to a separation of 10 thermal penetration depths, the agreement with theory improves. But at a smaller separation distance (i.e., 4 penetration depths), the agreement begins to diverge again (Figure 33). As the separation distance decreases from 3 cm to 4 thermal penetration depths, the observed temperature difference amplitude peak first increases then decreases. Concurrently, the slope of the temperature difference curve first steepens, then becomes more shallow. This indicates that there exists an optimum plate spacing distance.

The observed skewing is predicted by the theory (Figures 4 and 5) but at much higher amplitudes than those used in these experiments. In addition, theory predicts that the skewing is more pronounced in Helium than in Argon. Comparison of the results for these two gases at 162 dB pressure amplitude reveals that the skewing is equally severe. This fact, coupled with the fact that the onset of skewing occurs at much lower acoustic amplitudes than predicted, indicates that the reasons for the observed skewing are different from those presented earlier in this thesis.

It should be pointed out that the agreement between theory and experiment is quite good at all pressure amplitudes in regions near

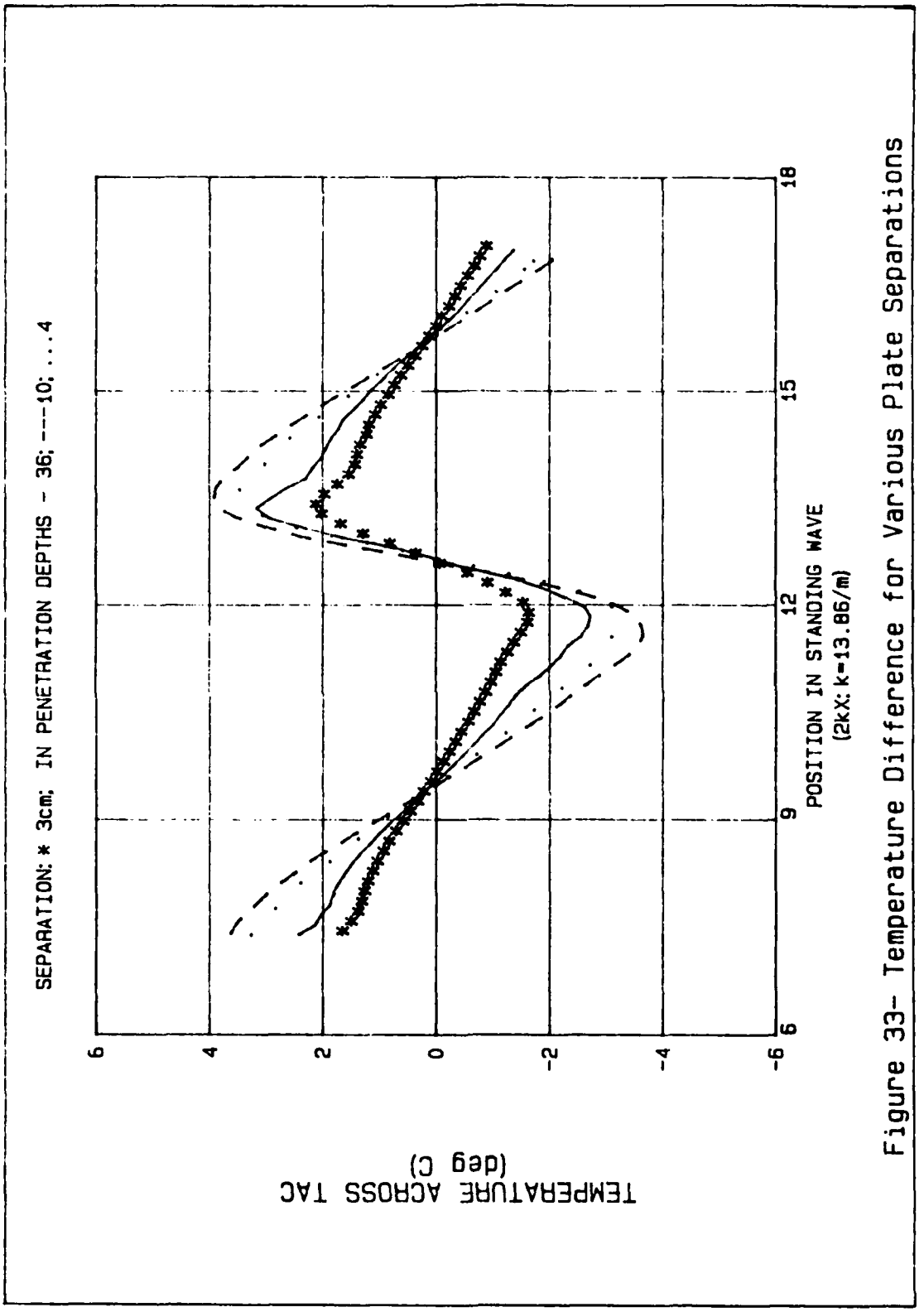

Figure 33- Temperature Difference for Various Plate Separations

the pressure antinode. In this region, the velocity amplitude is small and Γ is small. The discrepancy is worst in regions of large velocity amplitude or large Γ ($\approx$ 1). This observation points to possible regions of further investigation in order to explain the discrepancy.

Theory assumes that the TAC is short compared to the wavelength, so that the temperature gradient is constant along the plate and that acoustic dissipation due to the plate is small. In our measurements, the TAC was approximately 5 percent of the wavelength. Judging by the close agreement between the results and theory, the length of the TAC is sufficiently short for low amplitudes. At higher amplitudes, the short stack assumptions may be invalid, resulting in the observed discrepancies.

Still another possible reason for the discrepancies could be that the harmonics of the driving frequency are influencing the predicted heat flow. Using equation (12) and the acoustic amplitude of the second harmonic, measured to be some 20 dB lower than that of the resonance frequency, the temperature difference contribution was calculated. As can be seen in Figure 34, the maximum temperature difference due to the harmonic is only 0.04° C. Therefore, the second harmonic is not the cause of the discrepancies.

If we consider the theory as correct, and if it includes all the major thermoacoustic considerations, then some processes of non-thermal origin are responsible for the observed discrepancies from theory. One such non-thermal process is acoustic streaming.

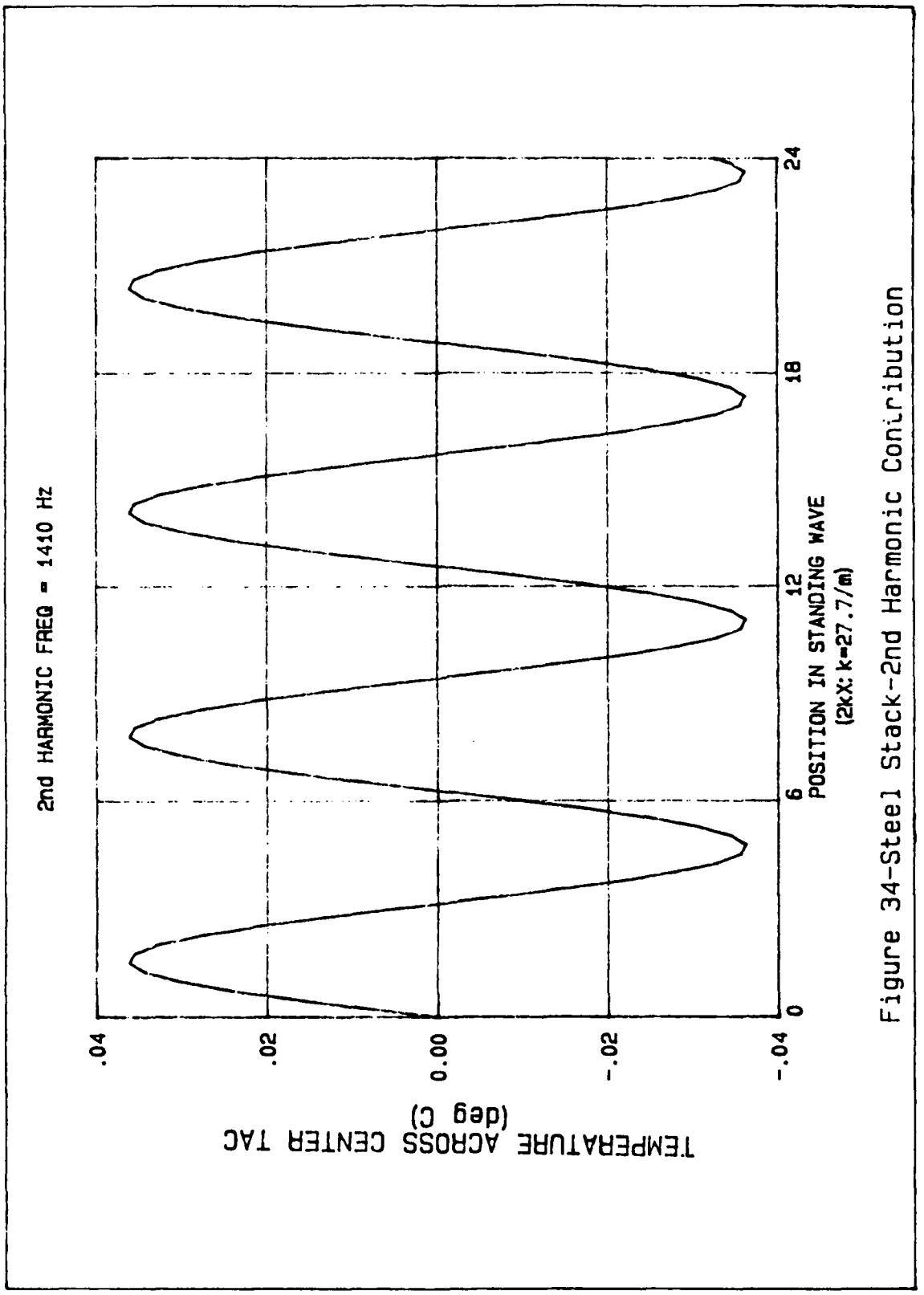

Figure 34-Steel Stack-2nd Harmonic Contribution

Because acoustic streaming occurs over any surface affected by an acoustic wave, we must consider two sources which could influence the heat transport. The first source is the streaming associated with the tube walls. This flow pattern is as discussed earlier (Figure 6). The second source is the streaming generated by the TAC plates themselves. It is assumed that the flow generated by the streaming would transport heat convectively, similar to what would occur if a stream of gas were blown across a plate having a temperature gradient across it. If the streaming effects of the tube are dominant, then the TAC temperature difference should vary along a diameter of the tube. This variation should be manifested as a difference minimum at the tube center and at tube walls, with a difference maximum midway between them. The measured diameter variations in the temperature difference do not demonstrate such behavior.

The measured data for both a single plate TAC and a stack, at both 150 and 162 dB acoustic pressure levels, is essentially constant, within experimental error, across the diameter (Figures 29-32). The magnitude of experimental error was determined by comparing the magnitude of the variations to those in successive data runs (Figure 13), and to the stability of the measured temperature differences (Figure 11). It is, therefore, concluded that acoustic streaming generated by the tube is not the cause of the discrepancies. Streaming effects on the plates occur within a few viscous penetration depths. The viscous penetration depth in these measurements is on the order of 70 μm. The thermocouple wires are 3 mils or 76.2 μm in diameter,

so the thermocouple joints are larger than the viscous penetration depth. Therefore, the effects of plate streaming could not be determined.

The changes in the observed data, when compared to the previously measured results, indicate an apparent motion of the TAC toward the driver. Even when the TAC is purposely positioned 1 cm closer to the driver, there still exists an apparent motion (Figures 35 and 36). The observed difference in the slopes in Figure 36 is due to the TAC starting at positions on opposite sides of the peak of the temperature gradient, which exists at the probe position. To determine the cause of this apparent motion, the precision of the probe and tube construction were studied, as were the variations in driving frequency, driving amplitude, and ambient temperature. These changes are considered to be of little consequence and the exact reasons for the apparent motion are undetermined.

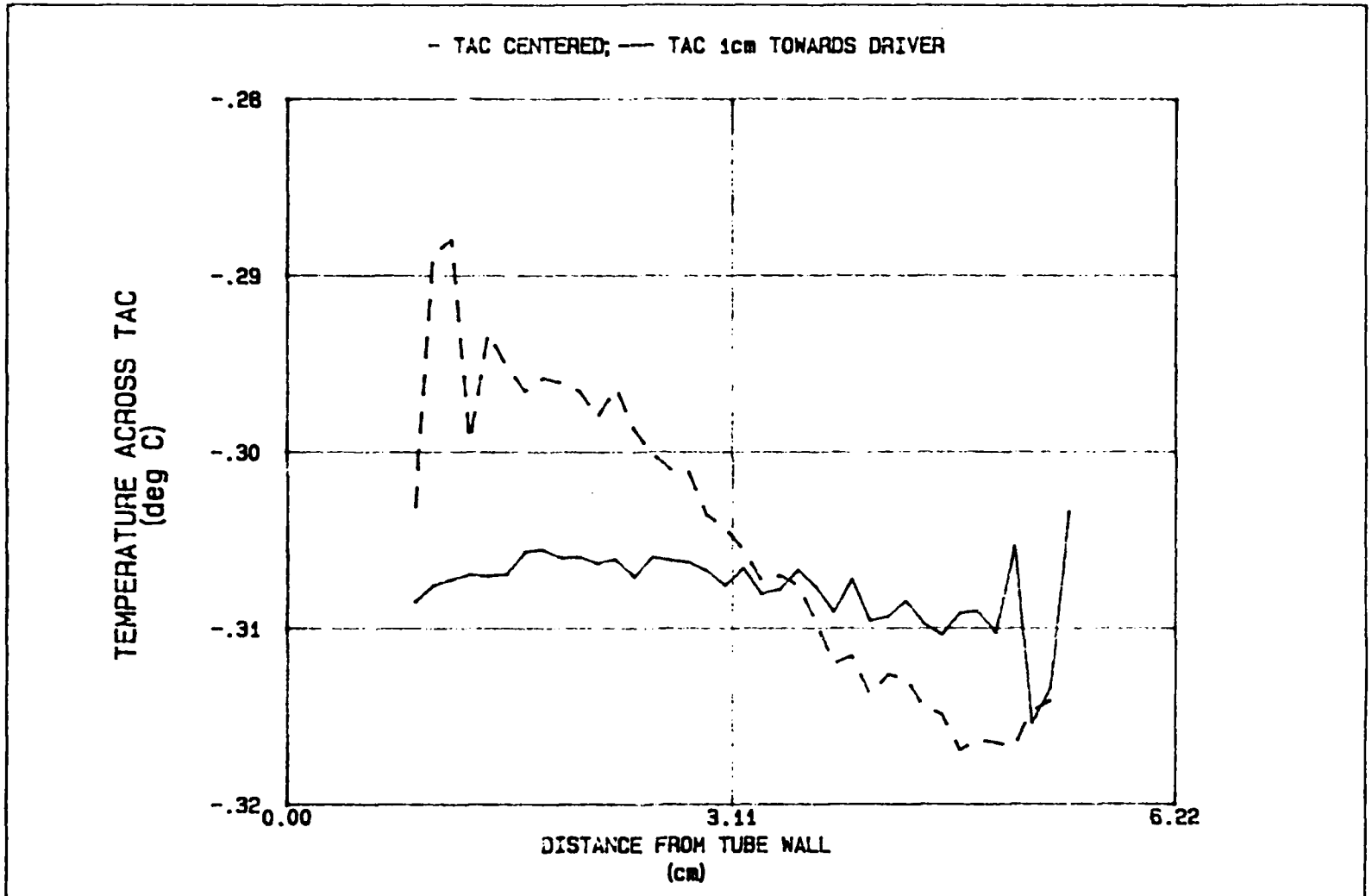

Figure 35 - Diametric Temperature Variation-Single TAC-150dB

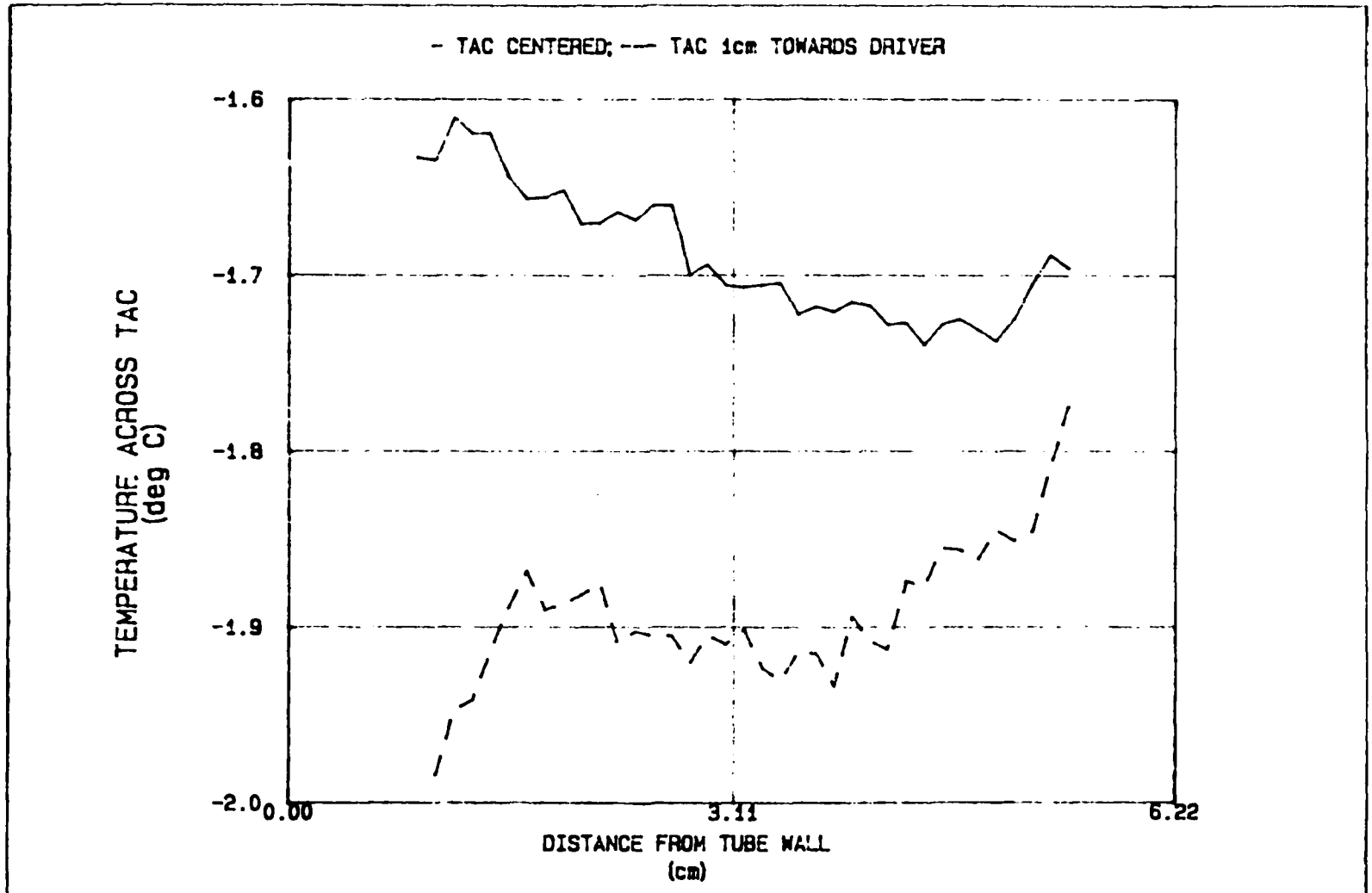

Figure 36 - Diametric Temperature Variation-Single TAC-162dB

VI. CONCLUSIONS AND RECOMMENDATIONS

It is concluded that the theory, for both a single plate and stack configurations, is valid at low acoustic amplitudes but not at higher amplitudes. Furthermore, assuming that all thermal processes have been included in the present theory, it is concluded that non-thermal processes, other than acoustic streaming in the resonant tube, are responsible for deviations from the theory. Finally, because of the discrepancies observed, especially at high acoustic amplitudes, it is concluded that a TAC would be a poor, or at least a very limited, acoustic power probe, as suggested by Wheatley [Ref. 2:p. 12], until a better understanding of high amplitude effects is achieved.

To better understand the processes involved and to determine the cause of the discrepancies, it is recommended that the experiments be repeated using:

a. Helium to maximize the thermoacoustic effects;

b. a shorter TAC to give better agreement with the short plate theory;

c. a phase-lock loop to stabilize the driving frequency; and

d. various plate separations in a stack to determine the optimum plate separation as a function of thermal penetration depth.

APPENDIX

PARTIAL LISTING OF THE PHYSICAL PROPERTIES OF ARGON AND HELIUM

TABLE I. PHYSICAL PROPERTIES OF ARGON [Ref. 4]

P	T	DEN	E	H	S	CV	CP	SOUND	VISC	COND
MPA	K	MOL/L	=== J/MOL ==		== J/MOL-K ==			M/S	PA-S E+6	MW/M-K
.107	290.00	.044	3609.	6018.	153.7	12.5	20.8	317.	22.3	17.4
.107	291.00	.044	3622.	6039.	153.8	12.5	20.8	318.	22.3	17.5
.107	292.00	.044	3634.	6060.	153.8	12.5	20.8	318.	22.4	17.5
.107	293.00	.044	3647.	6081.	153.9	12.5	20.8	319.	22.5	17.6
.107	294.00	.044	3659.	6102.	154.0	12.5	20.8	319.	22.5	17.6
.107	295.00	.044	3672.	6123.	154.0	12.5	20.8	320.	22.6	17.7
.107	296.00	.044	3684.	6143.	154.1	12.5	20.8	321.	22.6	17.7
.107	297.00	.043	3697.	6164.	154.2	12.5	20.8	321.	22.7	17.8
.107	298.00	.043	3709.	6185.	154.2	12.5	20.8	322.	22.8	17.8
.107	299.00	.043	3722.	6206.	154.3	12.5	20.8	322.	22.8	17.9
.107	300.00	.043	3734.	6227.	154.4	12.5	20.8	323.	22.9	17.9

TABLE II. PHYSICAL PROPERTIES OF HELIUM [Ref. 4]

P	T	DEN	E	H	S	CV	CP	SOUND	VISC	COND
MPA	K	MOL/L	=== J/MOL ==		== J/MOL-K ==			M/S	PA-S E+6	MW/M-K
.107	290.00	.044	3617.	6029.	125.0	12.5	20.8	1002.	19.47	151.3
.107	291.00	.044	3629.	6050.	125.1	12.5	20.8	1004.	19.52	151.7
.107	292.00	.044	3642.	6071.	125.2	12.5	20.8	1006.	19.57	152.0
.107	293.00	.044	3654.	6091.	125.2	12.5	20.8	1008.	19.61	152.4
.107	294.00	.044	3666.	6112.	125.3	12.5	20.8	1009.	19.66	152.7
.107	295.00	.044	3679.	6133.	125.4	12.5	20.8	1011.	19.70	153.0
.107	296.00	.043	3691.	6154.	125.4	12.5	20.8	1013.	19.75	153.4
.107	297.00	.043	3704.	6175.	125.5	12.5	20.8	1014.	19.79	153.7
.107	298.00	.043	3716.	6195.	125.6	12.5	20.8	1016	19.84	154.1
.107	299.00	.043	3729.	6216.	125.6	12.5	20.8	1018.	19.88	154.4

LIST OF REFERENCES

1. Wheatley, John, T. Hofler, G. Swift, and A. Migliori, "An Intrinsically Irreversible Thermoacoustic Heat Engine," Journal of the Acoustical Society of America, Vol. 74 (1), July 1983.

2. Wheatley, John, Gregory W. Swift, and Albert Migliori, The Natural Heat Engine, Los Alamos Science, Fall 1986.

3. Weast, Robert C., ed., CRC Handbook of Chemistry and Physics, 61st ed., Boca Raton, Florida: CRC Press Inc., 1980.

4. McCarty, R. D., Interactive Fortran IV Computer Programs for the Thermodynamic and Transport Properties of Selected Cryogens, Washington D. C.: NBS Technical Note 1025, National Bureau of Standards, 1980.

5. McCarty, R. D., Thermophysical Properties of Helium-4 From 2-1500 K With Pressures to 1000 Atmospheres, Washington D. C.: NBS Technical Note 631, National Bureau of Standards, 1972.

6. Lighthill, James, Waves in Fluids, New York: Cambridge University Press, 1978.

7. El-Hakeem, A. S., "Velocity of Sound in Nitrogen and Argon at High Pressures," Journal of Chemical Physics, Vol. 42, No. 9, May 1965.

8. Moldover, Michael, James Mehl, and Martin Greenspan, "Gas-Filled Spherical Resonators: Theory and Experiment," Journal of the Acoustical Society of America, 79 (2), February, 1986.

INITIAL DISTRIBUTION LIST

		No. Copies
1.	Library, Code 0142 Naval Postgraduate School Monterey, California 93943-5002	2
2.	Department Chairman, Code 61 Department of Physics Naval Postgraduate School Monterey, California 93943	1
3.	Professor A. Atchley, Code 61AY Naval Postgraduate School Monterey, California 93943	3
4.	Dr. T. J. Hofler, Code 61HF Naval Postgraduate School Monterey, California 93943	1
5.	Professor S. Garrett, Code 61GX Naval Postgraduate School Monterey, California 93943	1
6.	DPED National Defence Headquarters Ottawa, Ontario Canada K1A 0K2	2
7.	Commandant ATTN: Dean, Science and Engineering Royal Roads Military College FMO Victoria, British Columbia Canada V0S 1B0	2
8.	Mr. and Mrs. Cecil Muzzerall Welsford Post Office Queens County, New Brunswick Canada E0G 3G0	1

9. Captain Michael Muzzerall — 3
301 Daniel Place
Victoria, British Columbia
Canada V9C 1W2

10. Lieutenant R. Middleton — 1
141 John Street
Hauppauge, New York 11787

11. Dr. G. W. Swift — 1
Condensed Matter & Thermal Physics (P-10)
Los Alamos National Lab
P. O. Box 1667/MS 764
Los Alamos, New Mexico 87545

12. Dr. L. E. Hargrove — 1
Physics Division, Code 1112
Office of Naval Research
800 N. Quincy Street
Arlington, Virginia 22217

13. Defense Technical Information Center — 2
Cameron Station
Alexandria, Virginia 22304-6145

END

FEB.

1988

DTIC